Project no.:
019809

Project acronym:
NextGenBioWaste

Project title:
Innovative demonstrations for the next generation of biomass and waste combustion plants for energy recovery and renewable electricity production

Instrument: Integrated project

Thematic priority: 6.1.3.1.4

Start date of project: 2006-02-24

Duration: 4 years

D 2.6.24
Particle deposition in the boiler of waste fired plants (GKS)

Revision [draft]

Due date of deliverable: 2009-10-23
Actual submission date: 2009-10-23

Organisation name of lead contractor for this deliverable: GKS

Project co-funded by the European Commission within the Sixth Framework Programme (2002-2006)		
Dissemination Level		
PU	Public	X
PP	Restricted to other programme participants (including the Commission Services)	
RE	Restricted to a group specified by the consortium (including the Commission Services)	
CO	Confidential , only for members of the consortium (including the Commission Services)	

Deliverable number:	D 2.6.24
Deliverable name:	Particle deposition in the boiler of waste fired plants
Work package:	WP 2.6 Boiler Optimisation/Design – Demonstration
Lead contractor:	GKS

Status of deliverable		
Action	**By**	**Date** (yyyy-mm-dd)
Submitted (Author(s))	Ragnar Warnecke	2009-10-23
Verified (WP-leader)	Robert van Kessel (KEMA)	2010-01-22
Approved (SP-leader)	Peter Paul van 't Veen (TNO)	2010-??-??

Author(s)			
Name	**Organisation**	**E-mail**	**Tel**
Ragnar Warnecke	GKS	Ragnar.warnecke@gks-sw.de	+49(9721)6580-120
Müller, Volker	GKS	volker.mueller@gks-sw.de	+49(9721)6580-125
Weghaus, Martin	Weghaus GmbH	mene@weghaus.de	+49 (931) 2075064

Abstract

Excepted knowledge is that corrosion of superheaters is caused by chlorine. In former times the gaseous phase had been in the focus for explaining the corrosion processes in these areas. Newer investigations of GKS had shown, that the mainly responsibility is at aerosols respectively at particles which contain chlorine. A very specific measurement system for particles had been developed which is described here. The measurements delivered a particle size distribution in the four different passes of the boiler. Using this particle distribution there had been made calculations by computational fluid dynamics (CFD). Within these calculations the sticking of the particles on the superheater tubes had been simulated while taking into account the different separation models. To be close to realistic boundary conditions a "morphing" mesh had been integrated into the commercial CFD code "CFX".

The results show an absolutely realistic deposition which is very close to what can be seen in the plant. This leads to much more information about the separation mechanisms and the processes at the superheater tubes. A reverse information is that not every class particles can take part on the corrosion process. Especially the very small particles pass the superheater tube without having a chance to stick there, that means, that they can not influence the corrosion process although they transport a high amount of chlorine. This leads to a concentration on larger particles as the "bad guys" concerning corrosion.

This information is useful to understand the corrosion mechanism in more detail. Finally this will lead to a higher availability. The gained knowledge can also be used in the design of new high efficient waste incinerators.

Version history (not to be used if Track version is used in eRoom).
To be deleted before final version is converted to PDF-format

Date	Version	Author(s)	Comments
2009-10-23		Ragnar Warnecke	DRAFT

TABLE OF CONTENTS

Page

1 INTRODUCTION

In former times waste was a source of illness and pestilence. Incineration is the appropriate measure for:

1. inertisation of waste to a non-dangerous, hygienic matter
2. minimising its volume (to about 10 % of the former volume)
3. gaining energy (electric power and heat) and
4. preparing for suitable recycling (metals etc.).

Waste incineration under controlled conditions in a technical plant is part of the waste handling for more than one hundred years now and seems to be the appropriate technique for the future. While the combustion of more or less homogenous fossil energy material (i.e. gas, oil, lignite, coal) is investigated extensively in the last decades, the understanding of the combustion process for strongly heterogeneous materials as waste, RDF, biomass etc. is rudimental.

In the plants with heterogeneous fuel a lot of problems can occur: These can be for example the stability of the combustion itself, the release of corrosive species into the boiler and of deposit causing particles in the combustion chamber and boiler.

Within this part of the NextGenBioWaste project a more detailed description of the processes in combustion chamber and boiler has to be figured out. While the simulation of the majority components of the combustion process is state of the art, the behaviour of the minority components is hardly to be foreseen. This deliverable shows how a very detailed description especially of the aerosols, which are responsible for corrosion and deposits and by that for a decrease of availability and less efficiency, can be occurred.

2 PARTICLES IN THE BOILER OF WASTE-TO-ENGERGY PLANTS

The particles in WtE-plant have 2 substantial sources.
The 1st source is the release of solid particles from the bulk mass of waste during the transportation on the grate, while the waste is dried, pyrolised, gasified and combusted. The primary air carries these particles out of the bed and the raw flue gas drives them through the passes of the boiler.

The 2nd source is in situ formed particles, as a result of mainly over saturation the gaseous species which form very fine nuclei (a few nm in diameter).

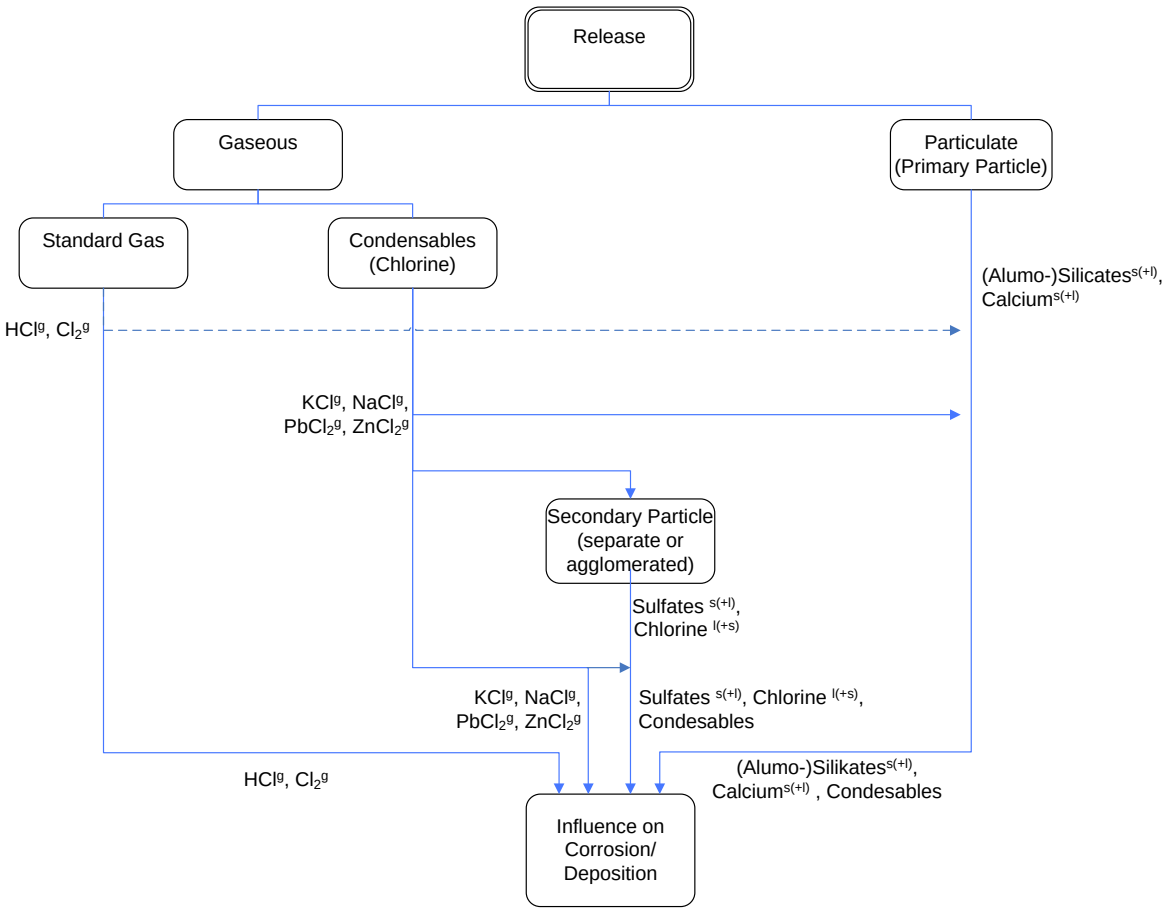

Fig. 2.1 Chlorine phases from fuel bed to superheater tube

The particles of both sources will change along the way through the boiler by several effects (Fig. 2.1).

The main effects influencing the particle during their flight through the passes of the boiler are:

1. Particle nucleation and growth by condensation
2. Particle agglomeration
3. Particle depositing on heat transfer surfaces.

In the following these mechanisms will be presented in theory and the practical measurement in practise.

2.1 Particle growth by condensation

Similar to the formation of in situ particles from the waste bed, condensation take place while the flue gas on its way through the passes of the boiler is cooled by the water cooled tubes. Partially the condensates will attach to the surface of existing particle. Because of the small mass of the particles the particles have more or less the same temperature as the surrounding gas. There is no need to sub cool the new condensate on the particles [Hind, 1982].

$$\frac{d}{dt}d_p = \frac{2v_m(p - p_{sat})}{\sqrt{2\pi m k_B T}} \quad for \;\; d_p < \lambda$$

$$\frac{d}{dt}d_p = \frac{4v_m D(p - p_{sat})}{k_B T \rho_p d_p} \quad for \;\; d_p > \lambda$$

d_p	particle-diameter
λ	mean free pass between inter molecule collision of flue gas (70 nm at S.T.P.)
v_m	volume of condensate molecule
k_B	Boltzmann-Constant
D	diffusion factor
m	mass of condensate molecule
ρ_p	density of condensate particle
p	(partial-)pressure
p_{sat}	saturation pressure
T	temperature
t	time

The saturation partial pressure increases for small particle diameters (Kelvin effect). For $d_p > \lambda$ the equations show that small particles grow faster than large. Further fine particles have a larger ratio of surface to volume the concentration of the condensate is higher on fine particles than on coarse.
Particularly at highly concentrated aerosols the heat transfer (release of condensation enthalpy) has to be regarded in the balance next to the mass-transfer. Corresponding applies to parallel chemical reactions (e.g. sulphating-reactions).

2.2 Particle growth by agglomeration

The size distribution of particles formed by combustion and / or condensation is not stable. The particles move randomly (Brownian motion), collide and form larger agglomerates gradually. This process is known as Brownian or thermal coagulation.
The change in mean particle size of x_V is shown in Fig. 2.1 by [Koch, 1996] as a result of numerical calculation. The higher the particle concentration (C_v [Vol. of particle/Vol. of gas]), the more rapid growth takes place. By massive dilution this undesirable effect can be suppressed for measurements.

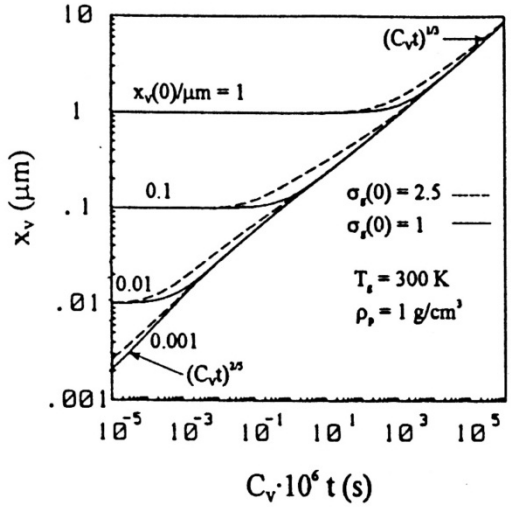

Fig. 2.1 Change of particle-diameter x_v as a function of particle-concentration caused by thermal agglomeration [Koch, 1996]

As one result of this calculation it can be seen, that after sufficiently long time the particle size depends no longer on the initial particle size whether they are a few microns or 1 nm in size. In parallel, the width of the size distribution trends to a given value (σ_g = 1.33, for the average particle distribution in the present case) and also originally existing differences in the composition of the particles disappear. The residence time in the boiler is about 3 – 30 seconds and the volume particle concentration about 0,5*10^-6.

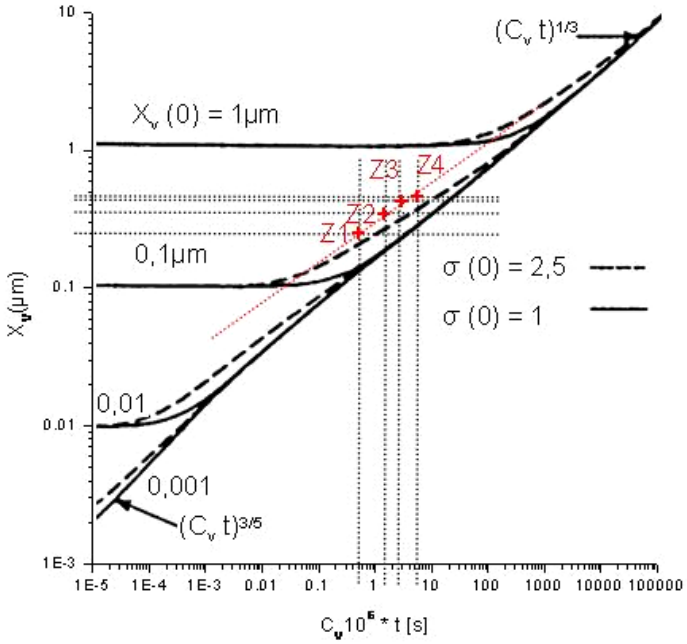

Fig. : 2.2: Change of particle-diameter calculated for the measured data (especially temperature)

The complexity of “particle-aging" by agglomeration is thus reduced significantly by this knowledge.

2.3 Particle measurement

The common measurement methods are described in the VDI 2066. There are both continuously (automatic) and discontinuously (manual) methods for measuring particles in flue gas. All methods should take place under iso-kinetic conditions especially for the measurement of particulate mater. The methods, in the following for to determine particulate emissions, are used to investigate the efficiency of particle separators, as reference methods for calibrating continuously recording dust content measurement equipment but are also used to get a better understanding of specific processes.

Continuously measuring of emissions is often required by legal demands and is mainly recording the data automatically. Here the most important methods are optical, radiative, extractive (incl. filtering) and tribo-electric methods.
Optical methods are based on transmission/opacity, extinction or scattered light. They become more and more important for monitoring dust emissions (but detection of species as SO2 or others as well). The other kinds of dust measuring methods are well proven too. All the mentioned methods deliver information about particle concentration only.
These methods for continuous measurement are suitable for temperatures up to a maximum of 300 °C but in general not for high temperatures as there are in the boiler of waste-to-energy or biomass plants. So for example it is not easy possible to work with optical transmission equipment on supersaturated gases.

Discontinuous measuring is almost always an extracting method. For this a sample stream of the gas is removed from the main gas flow. The contained particles are collected on filters or in complex measurement equipment. With recording the volume of the gas-sample and the mass of the collected particles the dust-content of the gas can be calculated. The mostly manual methods are well proven for simple conditions. At high temperatures, in severe ambiences and in presence of supersaturated gas all these methods are having problems during the measurement and can give results which have to be interpreted.

All of the above mentioned methods are uses to get an overall information of the total particle content and are done in more or less cold gases. For more precisely determination of the particle size distribution the sampled particles from discontinuous methods have to be analysed ex situ. For severe boundary conditions as high temperatures, corrosive atmosphere, high dust contents and supersaturated gases there are no standard methods available.

2.3.1 High temperature particle measuring

The measuring of particles at hot conditions shows a lot of challenges. Meanwhile, a variety of approaches to high-temperature samples and in different types of incinerators are published, for example [Mikannen, 1999], [Warnecke, 1999], [Tran, 2002], [Strand, 2004], [Obernberger, 2004], [Deuerling, 2005], and [Deuerling, 2009].

The high-temperature-probes can differ widely according to the demand. For a simple case an un-cooled silica-tube can be used. To avoid material destruction above 1000 °C the probe has to be cooled by arranging a casing tube around the probe and applying cooling air or water to that.

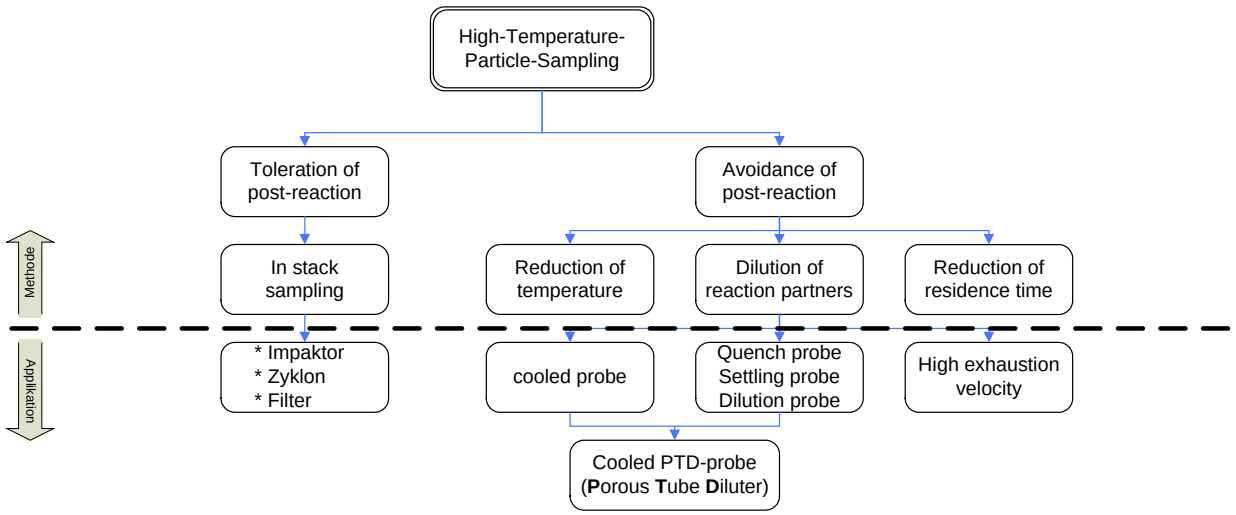

Fig. 2.3 Overview of high-temperature sampling methods

When the probe is stable against the ambiance in the boiler, it is most important to avoid post reactions of species and particles/aerosols and other interactions as e.g. agglomeration within the probe in order to get an artefact free sample.
After entering of the sample in the probe equipment there are different ways for further treatment of the sample according, if post-reactions are acceptable or not.
After getting the sample further treatment is necessary to avoid post-reaction within the sample.
In principle there are 3 variables to influence: temperature, concentration and reaction-time.

For reducing the temperature of the sample the probe has to be cooled. Dilution of the sample will decrease the concentration. The reaction-time can be influenced by the exhausting-velocity, but this can be contradictory to the requested isokinetic conditions. The separate treatments can also be combined.
Typical diluting devices used for sampling of aerosol at for high-temperature are diluting-tunnel, ejector-diluter, porous tube diluter (PTD), filtration diluter and rotating disk diluter. It is known that all diluter will influence the particle size distribution more or less. The temperature of the diluting gas and the moisture of the hot gas rank first. Ejector diluter show a loss of about 30 % for particle number compared to diluting tunnel and a shift to smaller particles. These losses are considered to sticking at the inlet nozzle. Diluting tunnel show a significant tendency for nucleation.
According to literature the PTD is the method with the least influence to the particle size distribution. But at low final temperature condensation has to be noticed.

Besides the probe, dilution and cooling the connecting pipes are another influence to the sample. There is no concrete valuation for this loss and shift effect.

3 PARTICLE MEASUREMENTS AT GKS

Since 2003 there had been developed a measurement equipment at GKS to take particle samples at temperatures up to 1.200 °C in the boiler and even in the combustion chamber. Partners of this development were GSF, Munich, and BIfA, Augsburg (see the PhD of [Deuerling, 2009]).

3.1 GKS-Particle measurement method

Over the last years a comprehensive sampling arrangement was developed at GKS. Parts of the measurement system are: Inlet nozzle with swan neck, porous tube diluter, pre-precipitating cyclone, two diluting ejectors, fine cyclone, condensation, drying and gas analysis. Behind the diluting ejectors there is an online particle measurement system with APS (atmospheric particle sizer) and an ELPI (electrical low pressure impactor).

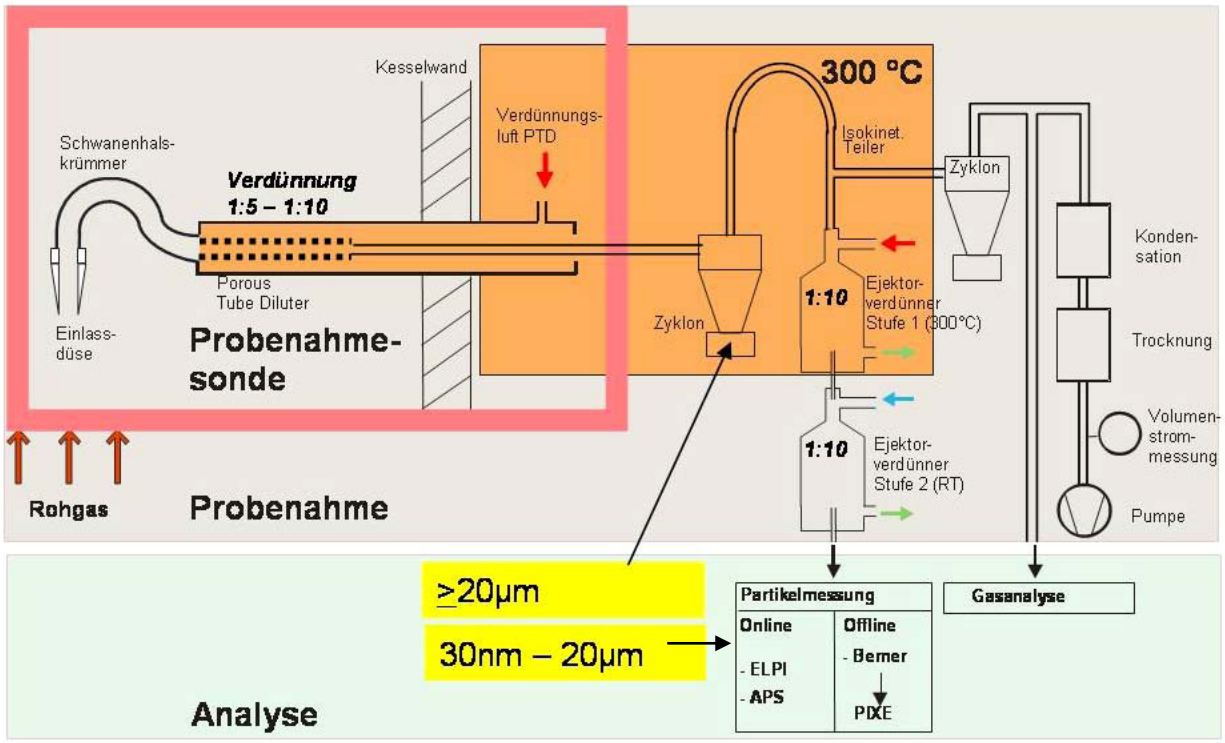

Fig. 3.1 GKS particle sampling method

In general the GKS-probe is an advanced porous tube dilutor (PTD). The probe will dilute the gas by a factor of about 5 - 10 in a porous tube diluter and cool down to 300 °C.

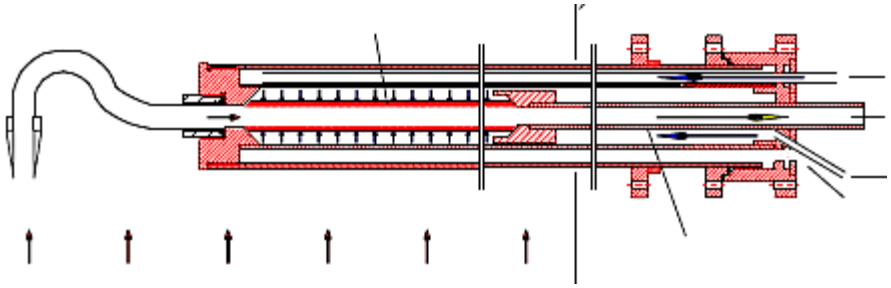

Fig. 3.2 GKS probe (raw gas from below – see arrows)

The probe is designed as a triple jacket probe with 3 cooling air lines. The outer jacket serves a supporting structure and stabilizes the whole temperature regime of the device.
The cooling jacket for the outer supporting tube will lead the cooling gas out of the boiler. This prevents an influence of a too high heat flux to the porous tube. The middle jacket will lead the preheated diluting air to the porous tube.

The next device is the cyclone, which is designed for a separation diameter of 25 μm.

Fig. 3.3 Cyclone for coarse fraction

After the cyclone there are two diluters before the gas enters the particle analysing equipment.
The total arrangement for measuring particles at high temperature can be seen in Fig. 3.4 below.

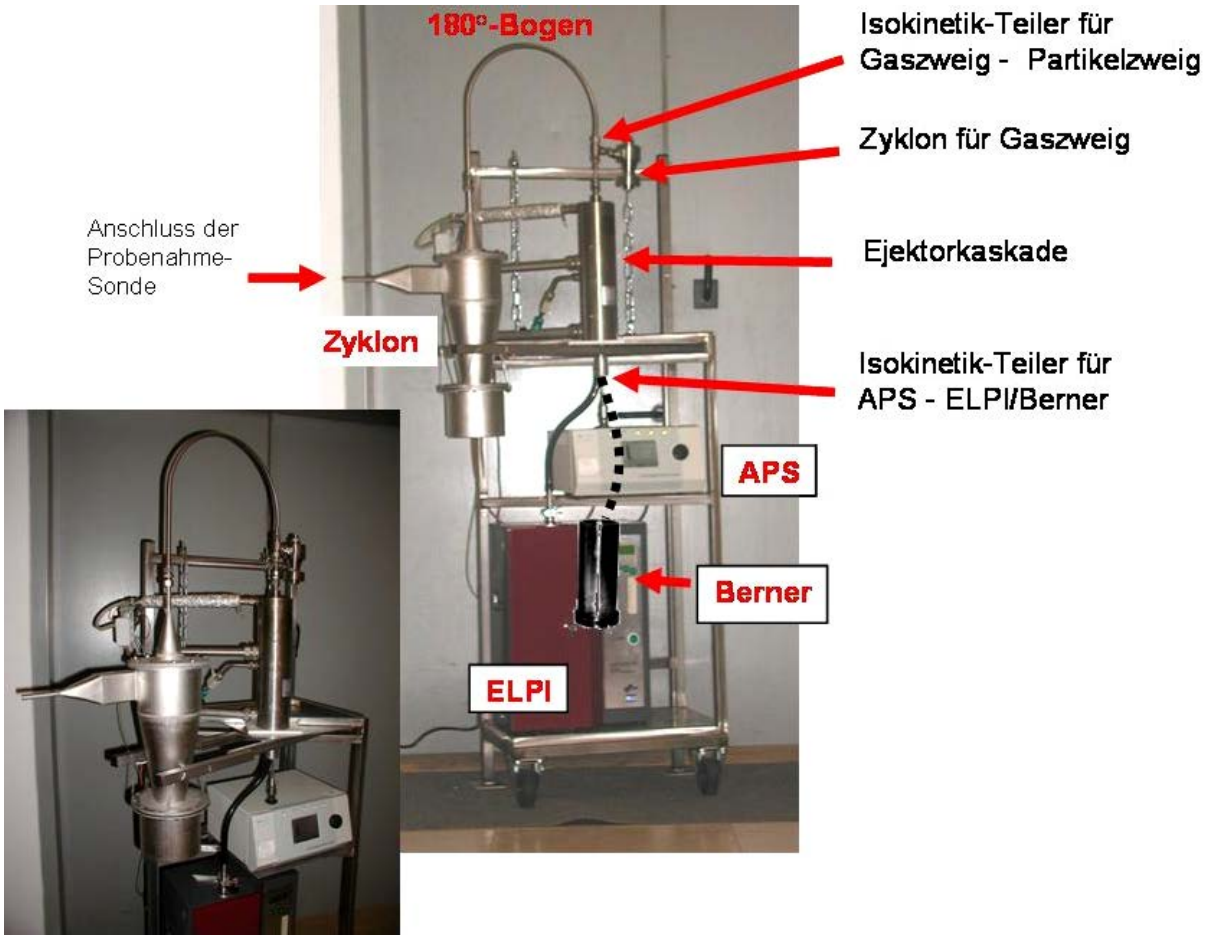

Fig. 3.4 Sampling and measuring system at GKS

The measuring devices for particle sizes are APS (Aerodynamic Particle Sizer), Berner-impactor and ELPI, for gas phase it is an FTIR (Fourier Transformed Infra-Red Analyser).
The ELPI (Electrical Low Pressure Impactor) in principal is a low pressure impactor which will operate online, as well as the APS. The incoming particle are loaded electrical and are separated at the impactor cascade by 12 size fractions. On impact the particle discharge and the charge is registered.
The size fractionation is caused by inertia of the particles.

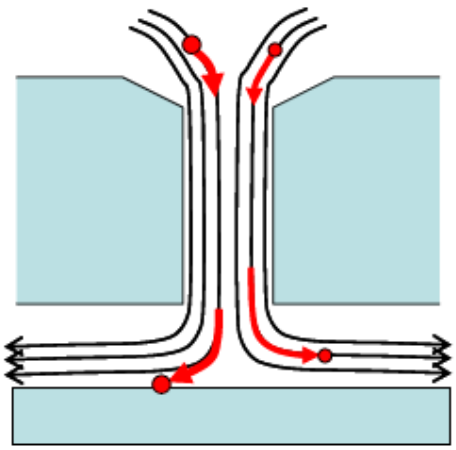

Fig. 3.5 Principle effect at fractionation step in an ELPI.

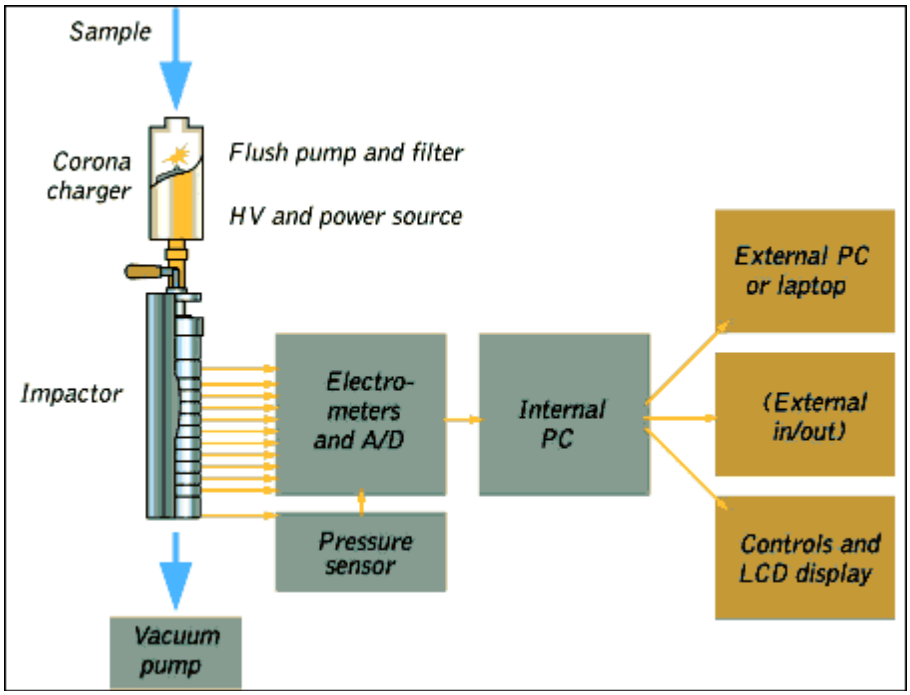

Fig. 3.6 Scheme ELPI

The APS (Aerodynamic Particle Sizer) characterizes an aerosol in respect to number- and mass concentration distribution in a range of 0.58 - 20 µm.

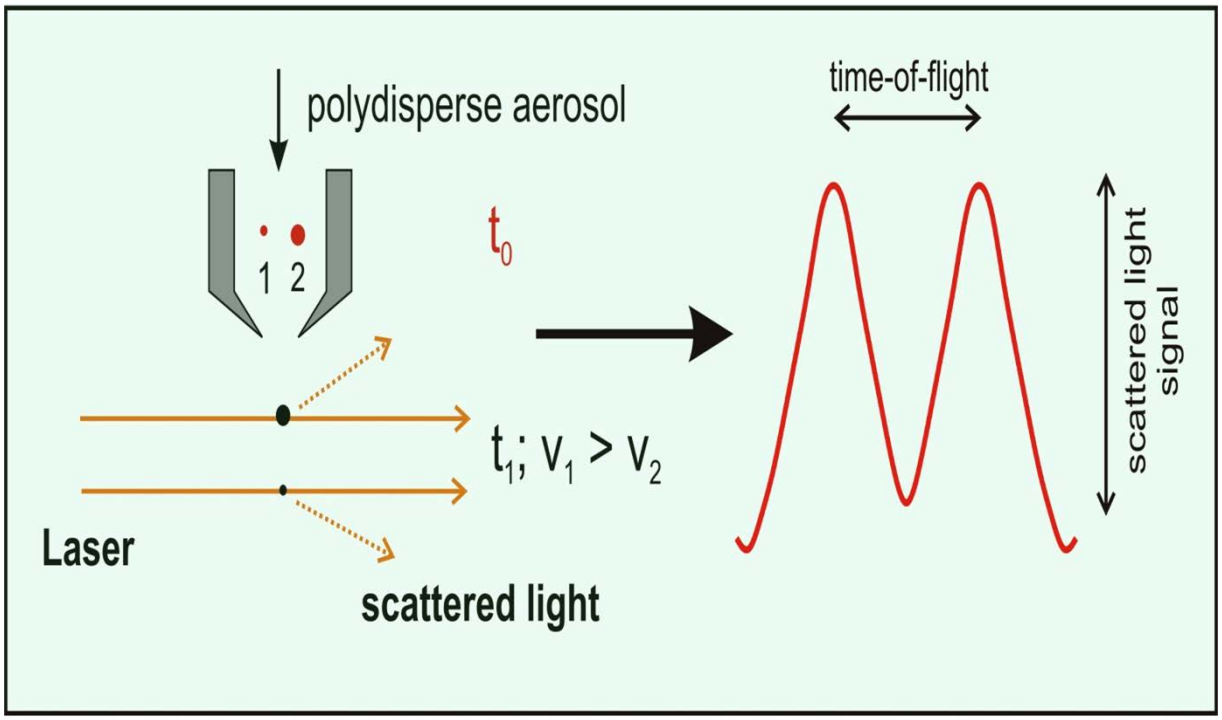

Fig. 3.7 APS principle method

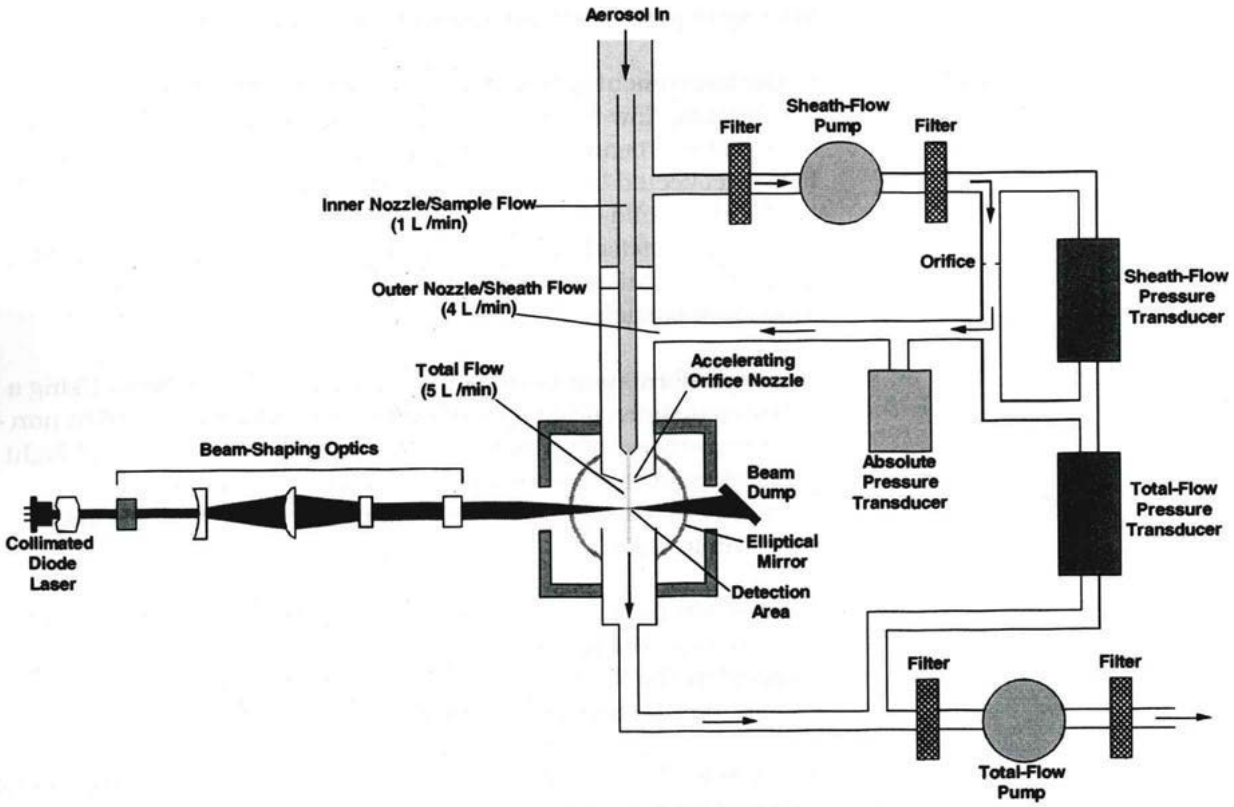

Fig. 3.8 Scheme APS

The principle of measuring is the acceleration of particles in a channel and subsequent determination of final velocity. So it belongs to the group of travelling time spectrometer.

The Berner-low pressure impactor make use of the impaction-principle to get a logarithmical separation by aerodynamically diameter. The resolution is 62,5 nm to 10 µm with 8 steps.

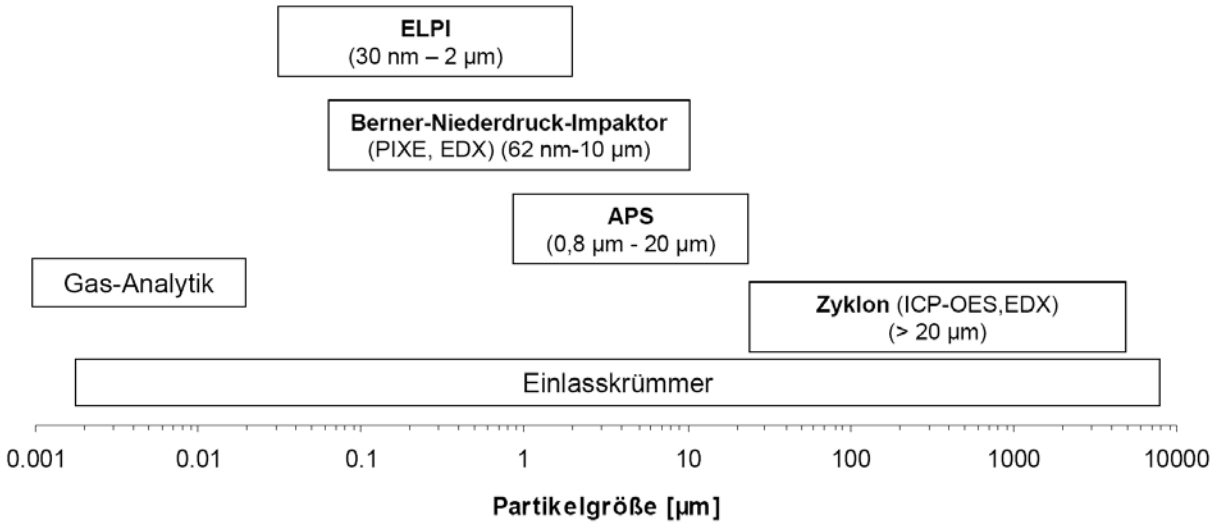

Fig. 3.9 Measuring ranges of used methods

3.2 Results

The above mentioned equipment has been deployed to analyse particles collected in several passes in the GKS plant. The size fractional particle distribution is shown in Fig. 3.10 as standardized number concentration. The range of measured numbers is of about 15 magnitudes.

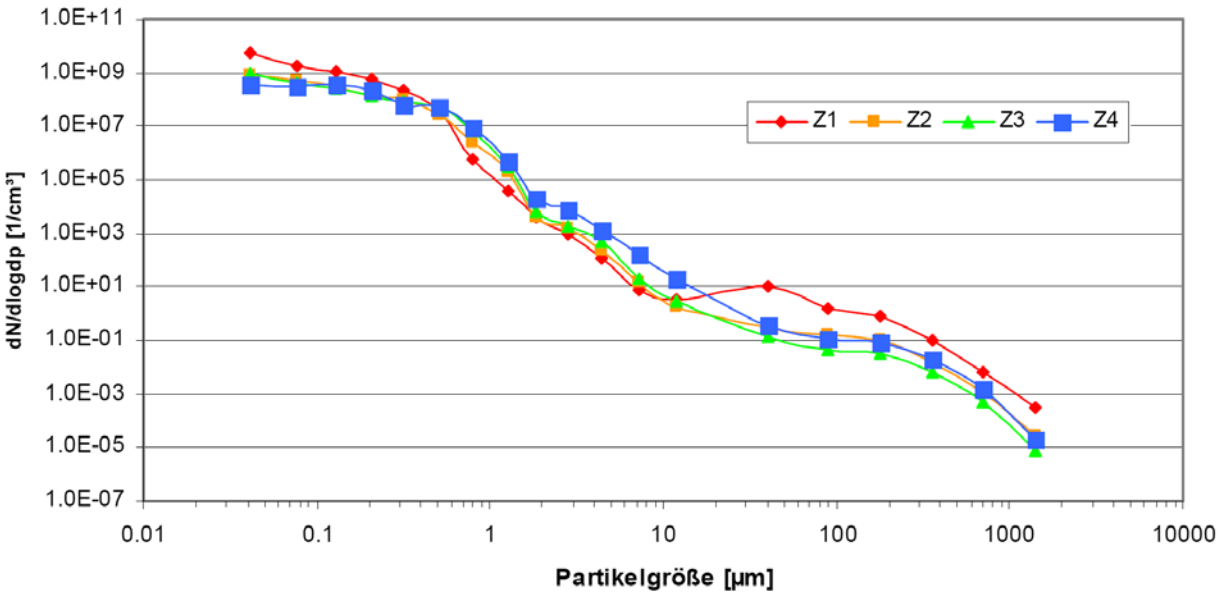

Fig. 3.10 Particle-number distribution as function of particle size and parameter of different passes in the boiler.

Figure 3.11 shows the mass concentrations as function of the particle diameter. Here clearly a bimodal distribution is found. This has been reported earlier in literature for similar combustion systems. [Warnecke, 1999]

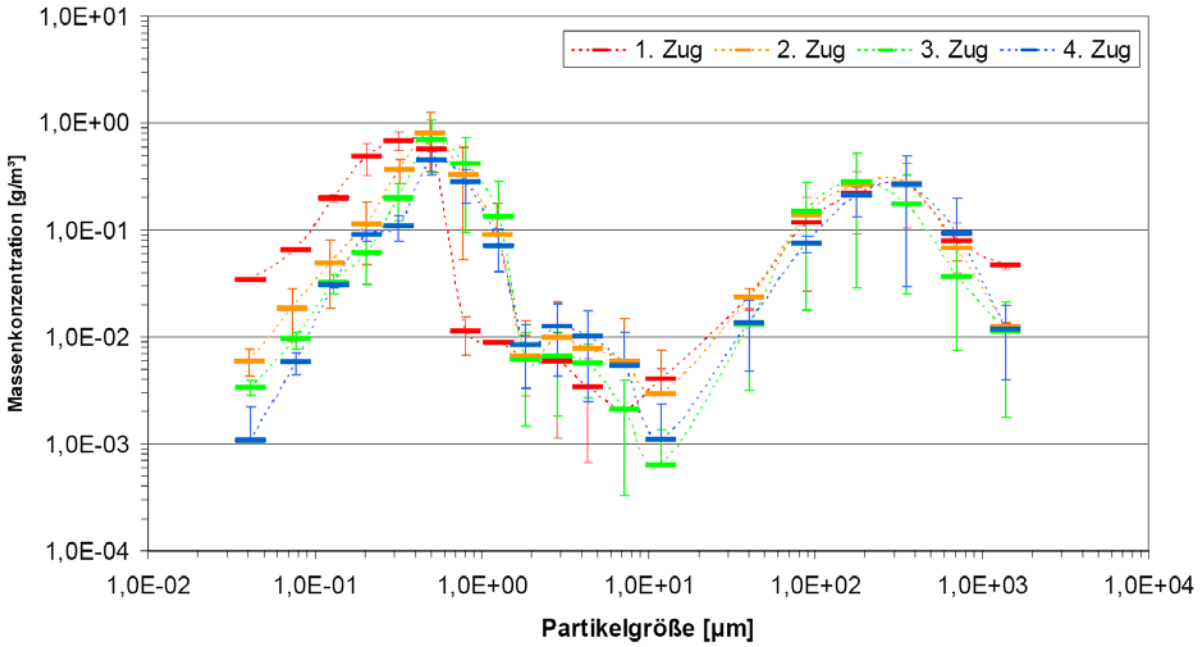

Fig. 3.11 Particle-mass distribution as function of particle size and parameter of different passes in the boiler.

The particle mass distribution is given in the following table (Table 3.1).

Table 3.1: Concentration of particles through the passes of the boiler in Line 11 at GKS

			Pass 1		Pass 2		Pass 3		Pass 4	
	No. of measurements: →		n=2		n=8		n=4		n=2	
Measurement methode: ↓	Class of particle size: ↓	Average size: [µm]	Average [mg/Nm3]	Standard Deviation [mg/Nm3]	Average [mg/Nm3]	Standard Deviation [mg/Nm3]	Average [mg/Nm3]	Standard Deviation [mg/Nm3]	Average [mg/Nm3]	Standard Deviation [mg/Nm3]
ELPI	Stage1	0,041	3,34E-02	8,23E-04	5,98E-03	1,70E-03	3,36E-03	5,23E-04	1,07E-03	1,17E-03
ELPI	Stage2	0,0773	6,60E-02	2,84E-04	1,85E-02	9,48E-03	9,50E-03	1,70E-03	5,80E-03	1,40E-03
ELPI	Stage3	0,1308	1,98E-01	1,55E-02	4,92E-02	3,05E-02	3,19E-02	6,44E-03	3,03E-02	1,23E-03
ELPI	Stage4	0,2061	4,86E-01	1,58E-01	1,14E-01	6,70E-02	6,00E-02	2,90E-02	8,97E-02	1,08E-02
ELPI	Stage5	0,318	6,85E-01	1,33E-01	3,66E-01	9,49E-02	1,98E-01	7,49E-02	1,08E-01	2,92E-02
ELPI	Stage6	0,5028	5,68E-01	2,99E-02	7,97E-01	4,43E-01	7,04E-01	3,57E-01	4,41E-01	1,19E-01
ELPI	Stage7	0,8	1,11E-02	4,36E-03	3,23E-01	2,71E-01	4,14E-01	3,18E-01	2,76E-01	9,74E-02
ELPI	Stage8	1,2728	8,89E-03	0,00E+00	8,85E-02	8,93E-02	1,34E-01	1,51E-01	7,10E-02	3,03E-02
APS	Stage18	1,843	6,54E-03	3,68E-03	6,65E-03	7,63E-03	6,12E-03	4,67E-03	8,25E-03	4,97E-03
APS	Stage24	2,839	5,93E-03	4,81E-03	9,78E-03	1,21E-02	6,53E-03	4,74E-03	1,23E-02	7,99E-03
APS	Stage30	4,371	3,43E-03	2,77E-03	7,66E-03	9,89E-03	5,65E-03	2,96E-03	9,94E-03	7,45E-03
APS	Stage37	7,234	2,09E-03	1,76E-03	5,88E-03	8,97E-03	2,10E-03	1,77E-03	5,30E-03	5,78E-03
APS	Stage44	11,97	4,02E-03	1,11E-03	2,91E-03	4,61E-03	6,26E-04	7,21E-04	1,11E-03	1,25E-03
Zyklon	Sieb0	40	2,34E-02	4,79E-03	2,32E-02	5,20E-03	1,30E-02	9,89E-03	1,34E-02	8,58E-03
Zyklon	Sieb1	89	1,16E-01	8,92E-02	1,35E-01	1,37E-02	1,48E-01	1,31E-01	7,42E-02	1,25E-02
Zyklon	Sieb2	177	2,20E-01	1,28E-01	2,65E-01	1,19E-02	2,76E-01	2,47E-01	2,08E-01	7,53E-02
Zyklon	Sieb3	354	2,67E-01	1,62E-01	2,72E-01	1,39E-02	1,74E-01	1,49E-01	2,61E-01	2,31E-01
Zyklon	Sieb4	707	7,77E-02	3,82E-02	6,65E-02	1,49E-02	3,68E-02	2,92E-02	9,28E-02	1,02E-01
Zyklon	Sieb5	1400	4,61E-02	3,00E-03	1,25E-02	9,08E-04	1,13E-02	9,50E-03	1,19E-02	7,91E-03
Sum:			3,20E+00	2,62E-01	2,96E+00	9,21E-01	2,56E+00	1,77E+00	2,05E+00	3,09E-01

4 PARTICLE DEPOSITION

For better understanding of technical plants, CFD simulation methods are a handsome instrument. Continuously improved computers enable better and more complex approaches. 10 years ago a simulation had to be as small as possible which lead to model with small dimension, rough discretisation and for further reduction with symmetry-assumptions. Now it is possible to simulate a complete boiler on a standard-PC.
Basis for the flow field describing CFD-methods is the solution of the Navier-Stokes equations for the simulation of laminar respectively turbulent flow. The results are detailed numerical descriptions for values like pressure, velocity, temperature or chemical reaction.

There are different approaches to the solution of Navier-Stokes. The DNS (direct numerical Solution) solves the Navier-Stokes itself. No empirical inputs are necessary, the solution has the character of an physical experiment. But different to a physical experiment DNS will provide all physical values, even non-measurable. The computational effort for that is immense, so the size of the models is hardly restricted.

The common CFD-packages use empirical models to solve subsets of Navies-Stokes. This leads to a simpler differential equation system which can be solved in trickle of time compared to DNS. In contrary to that advantage, a lack of correctness concerning description of turbulence, especially in more complex models, can be realized.

For the submitted work the commercial CFD-package ANSYS-CFX is used.

ANSYS-CFX provides methods for the simulation of interaction between particle und flow field amongst others. Based on this module particle deposition on tubes is implemented in this work package.

Regarding to particle deposition some work is done especially for wood- and straw-fired plants. Kaer [Kaer, 2001] has done some fundamental work for the sticking of ash-particles according to there composition and temperature. Similar work is done by Obernberger [Obernberger, 2004]. Both describe the gross deposition of flue-ash to the walls of a boiler. The resulting deposition-thickness has no influence to the flow-field as it is a numerical value.
Within this task the detailed deposition of particles is in the focus. With the deposition of particles the geometrical outline of the model will change. For that the deposit has a massive influence to the flow-field and this causes as a retroaction a change in new deposition. The deposition is fully coupled to the flow-field and geometry.

In boilers tube bundle heat exchanges are located, which are cross-flowed by the flue gas. Co-transported particles will be partially deposited on these tubes. For the build-up of deposit of particles three steps are necessary:

- Transport of particles close to the tubes (“flight”) (no focus in this deliverable)
- Transport of particles through the fluid boundary layer onto a tube (“touch down”)
- Adhesion to the surface of the tube or on existing deposit (“sticking”)

4.1 Theory of "Touch Down"

The transport through the fluid boundary layer to the wall is done by various mechanisms, which are described below:

- Diffusion
- Thermophoresis
- Gravitation:
  - Impaction (inertial separation) and
  - turbulent deposition
  - Sedimentation
- Electrophoresis
- Interception

Of these electrophoresis and interception can be more or less:

- The blocking effect is to be considered when the dimensions of the barrier and particles are in the same order of magnitude. This is in case of e.g. fibre filters.

- Electrical forces contribute effectively to the particle transport when external electric fields exist. This is the case in electrical separators.

4.1.1 Particle deposition by diffusion

Particle diffusion can be sketched as a series of Brownian motions and turbulent fluctuations. The formal description for particle diffusion is analog to molecular motion

$$j = -D\,\nabla c$$

The transport rate is proportional to the gradient of concentration and the diffusion coefficient D which is defined as follows:

$$D = \frac{k_B\,T\,C_C}{3\pi\,\eta\,d_p}$$

$$C_C = 1 + 2{,}514\,\frac{\lambda}{d_p} + \ldots.$$

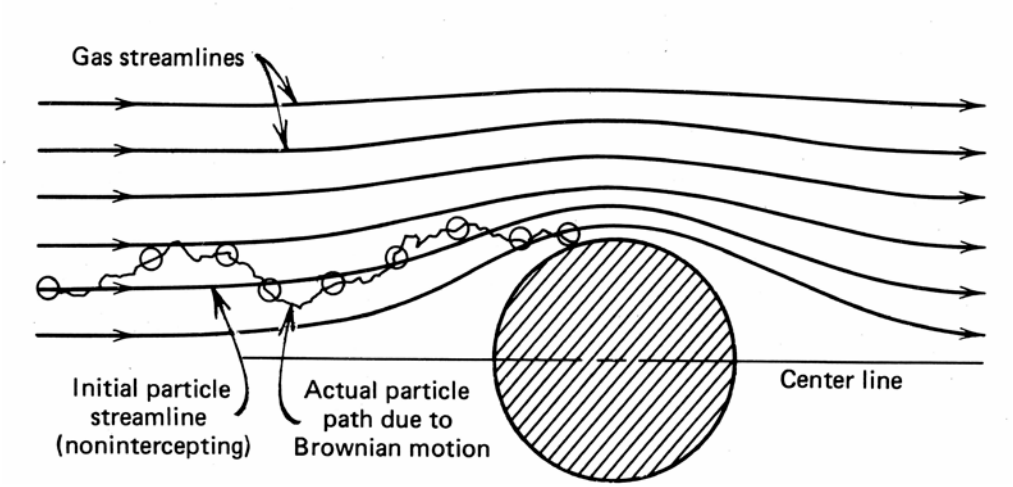

The Cunningham-correction C_c describes the transition from the continuum- to the molecular-flow. λ is the free length of gas (as standard $\lambda \approx 70$ nm). A figuratively value is the velocity for deposition v_{dep}.

$$v_{dep} = \frac{D}{\delta}$$

The more fine the particle, the greater the velocity for deposition will become. The correlation is dependent to the size-range linear or quadratic. Nano-particles are easy to separate from a gas hence.

The thickness of boundary layer for a cylinder [Fuchs, 1964] is:

$$\delta = 0{,}22 \square 0{,}4 \frac{d_{Rohr}}{\sqrt{Re_{Rohr}}}$$

The proportional constant increases from 0.22 at $\theta = 0°$ for the stagnation point to 0.28 at $\theta = 60°$ up to 0.4 at $\theta = 90°$. So the velocity of deposition varies along the perimeter of a tube nearly by factor 2.

4.1.2 Thermophoresis

Transport by thermophoresis can be understood as a consequence of Brownian motion of gas-molecules, which abut on the particle. Transport of particles will occur within a gradient of temperature.

A particle in a temperature-field will get following velocity [Hinds.1982]:

$$v_{th} = \frac{-0{,}55\ \eta\ \nabla T}{\rho\ T} \qquad d_p < \lambda$$

$$v_{th} = \frac{-3\pi\ C_C\ H\ \nabla T}{2\ \rho\ T} \qquad d_p > \lambda$$

Values ρ and η define the state of gas. Function H depends on d_p/λ and the ratio of conductivity of gas to particle.

Thermophoresis is no explication for species- and location-specific effect.

4.1.3 Impaction

Bigger particles cannot follow truly the streamlines because of inertia and impact to an obstacle.

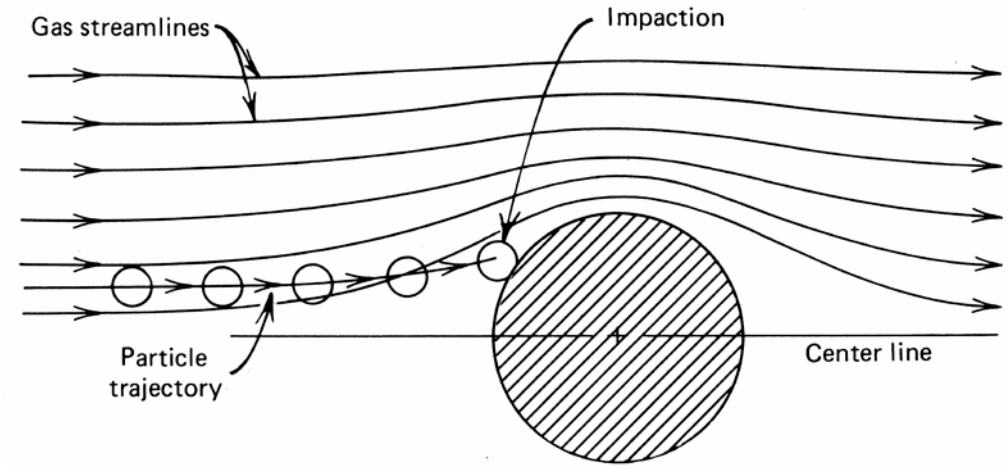

Fig. 4.1 Scheme for impaction

From all particles that move on an straight way to the tube just a part ε will reach the tube. ε is defined as [Fuchs, 1964]:

$$\varepsilon = \frac{\mathrm{Stk}^3}{\mathrm{Stk}^3 + 1{,}54\mathrm{Stk}^2 + 1{,}76}$$

The Stokes-number Stk is the stopping distance s_0 relating to the radius of tube.

$$\frac{1}{2} Stk = St = \frac{w_g}{g} \frac{u}{d_{tube}} = \frac{s_0}{d_{tube}}$$

$$w_g = \frac{(\rho_p - \rho_g)\, g\, d_p^2}{18\,\eta} C_C \qquad \mathrm{Re}_p < 1$$

So the particle diameter, which influences the behaviour in a deflected flow, is finally the stationary settling speed w_g.

The separation efficiency depends greatly on the particle diameter (Fig. 4.2).

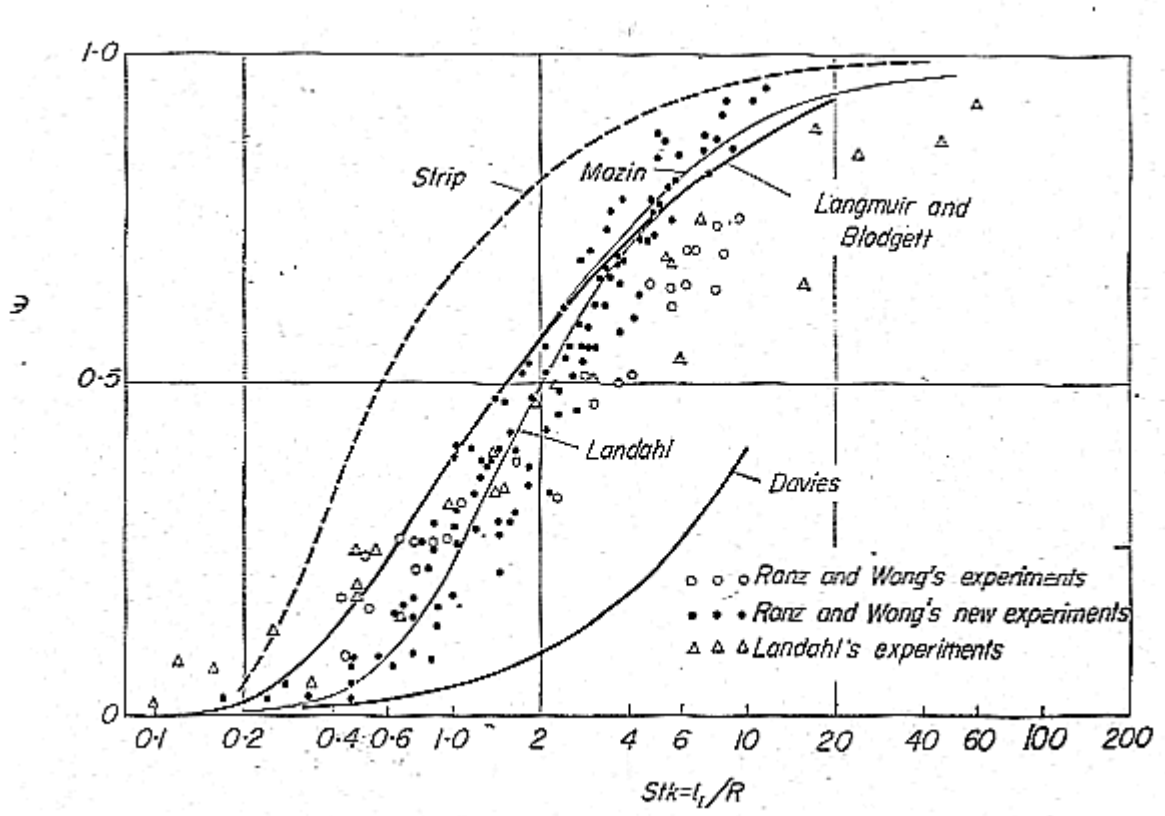

Fig. 4.2 Separation efficiency at a cylinder by impaction [Fuchs, 1964]

Obviously it is possible to separate particles by impaction to the windward side. But also here a strong dependency from the angle is noticeable. All particles coming to the tube will touch the stagnation point which considerable higher probability than they will reach the sides of the pipe.

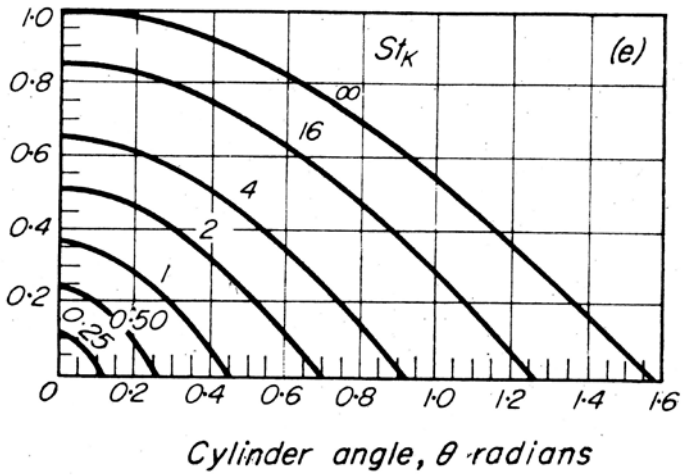

Fig. 4.3 Angle-dependence of separation efficiency at a cylinder by impaction [Fuchs, 1964]

4.1.4 Sedimentation

Noticeable sedimentation occurs in regions of low velocities. Particles are transported to that region by one or a combination of the fundamental effect. After reaching these regions the other effects will be of negligible importance causing the particles to sink by gravity.

4.2 Sticking

A solid particle will stick to a wall, if the elastic energy is smaller than the energy needed to overcome the adhesion force [Löffler, 1988]:

$$v_{krit} = \frac{1}{d_p} \frac{\sqrt{1-k_{el}^2}}{k_{el}^2} \frac{A}{\pi a_0^2 \sqrt{6 p_{pl} \rho_s}}$$

k_{el} part of elastic energy
A Hamaker-constant for van-der-Waals force
a_0 minimal contact distance
p_{pl} flow pressure

Even at ambient conditions the input values have a great uncertainty.
Particles of 10 µm can reflect at impact velocities over 10 cm/s.
In a first step the removal of particles from the surface has been neglected.

5 CFD-SIMULATION

The theory discussed in the previous chapter has been used to prepare submodels which can be used in the commercial CFD package CFX. In order to see what the value is of the model is, a principle CFD model has been setup. The model shows 5 pipes in flow direction. The arrangement is typical for a heat exchanger in the 3rd pass of boilers.

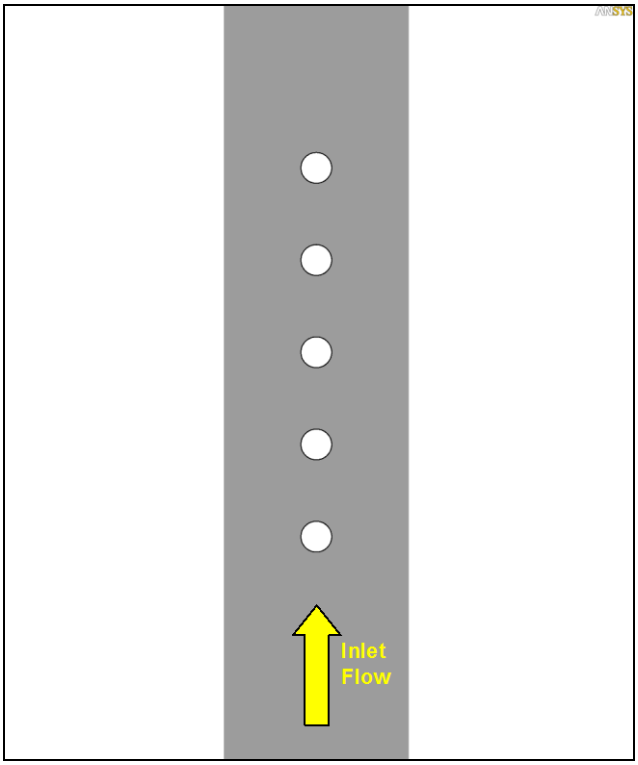

Fig. 5.1 Principle model

The model Boundary conditions:

- The simulation is quasi 2D and has periodic interfaces to get a certain influence from the virtual next pipe rows to the left and right.
- For the simulation a typical particle distribution and gas phase composition, temperature and pressure for the 3rd duct is chosen.
- During the real process, wear and soot blowing is applied to the deposit. The simulation does not incorporate that effect.
- Further there is no confirmed knowledge for the sticking of particles in WtE-plant. So within the simulation a modified Gauss probability is used as a first attempt for the sticking-probability.
- Condensation to the deposit is not regarded.

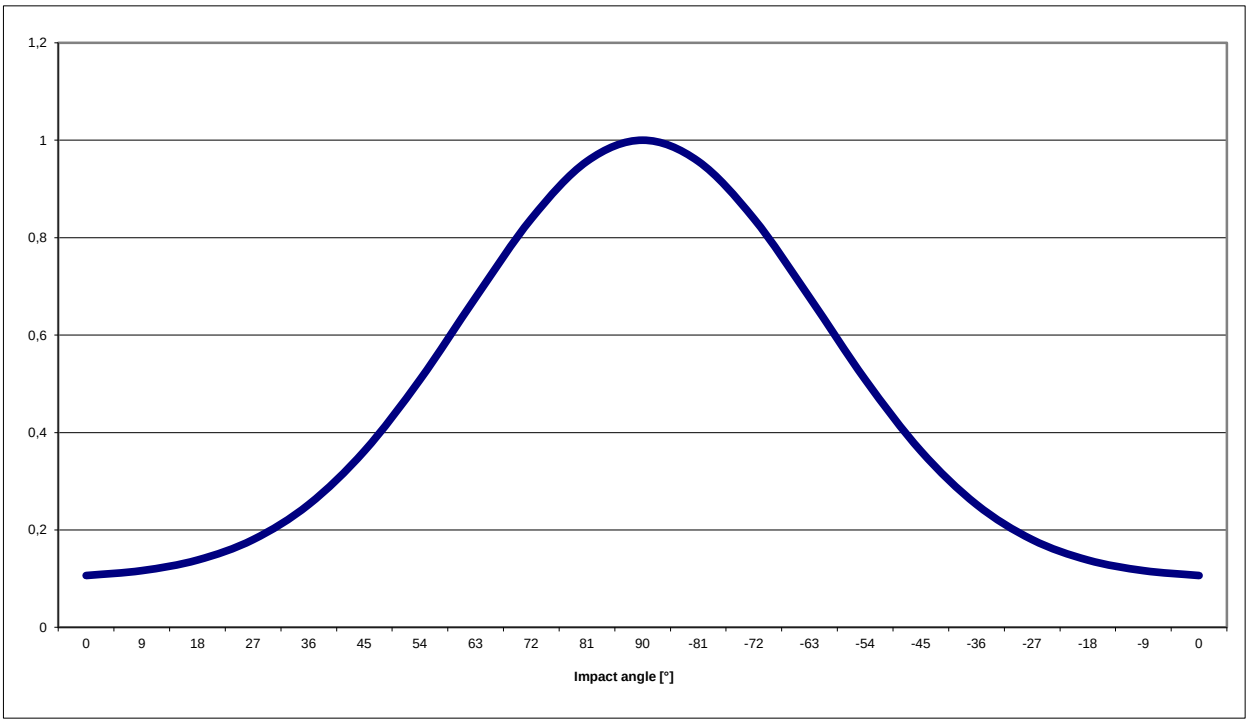

Fig. 5.2 Sticking probability distribution (44 % are under the curve = sticking; 56 % are above the curve = rebound)

Even at impact angles near to 0° which mean parallel flow to the line of the following tubes (in direction of the gas flow – i.e. the sides of the tubes) about 10 % of the particles stick to take in account the quite rough surface of the deposit.

The by time forming deposit will build a greater resistance for heat conduction. The local temperature of the deposit-surface will become closer to the temperature of gas. This results in decreased effect by thermophoresis.

5.1 Results:

To get a resolution of Karman-vortices the chosen time step for the transient run was 5E-4 seconds.

The results have to meet the observed geometry in the plant as shown in Fig. 5.3:

Fig. 5.3 Photography of deposits at a superheater in GKS plant

5.1.1 Velocities:

As expected the flow field shows distinctive Karman vortices. In particular it has to be marked, that the vortex-effect starts behind the second tube. This will trend a different behaviour in the gap between the 1st and 2nd tube.

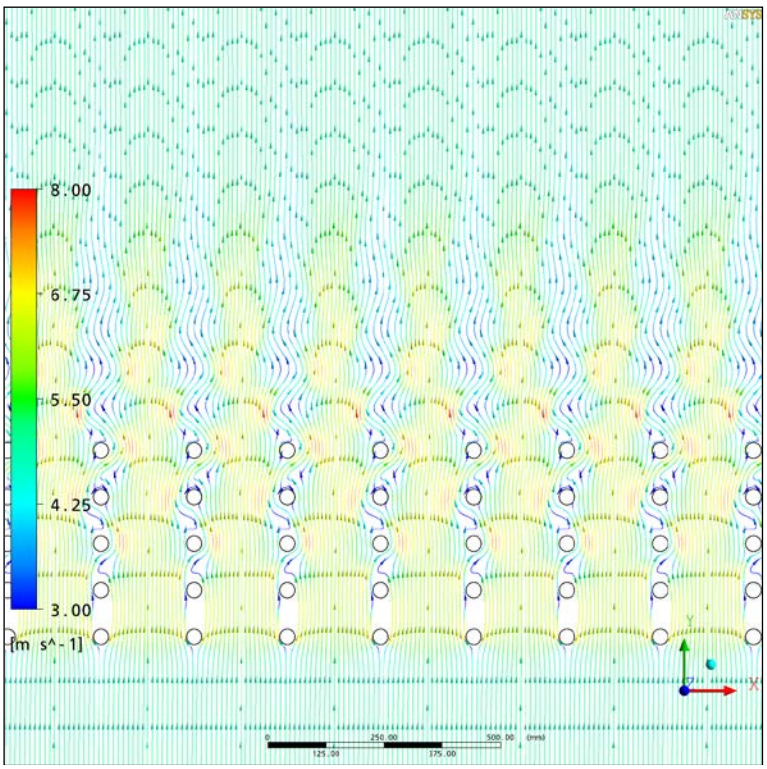

Fig. 5.4 Flow field for clean tubes

As described above the flow field will change with the formation of deposit. By the open area between the tubes will become smaller the vortex-fluctuation to this region will diminish and finally disappear.

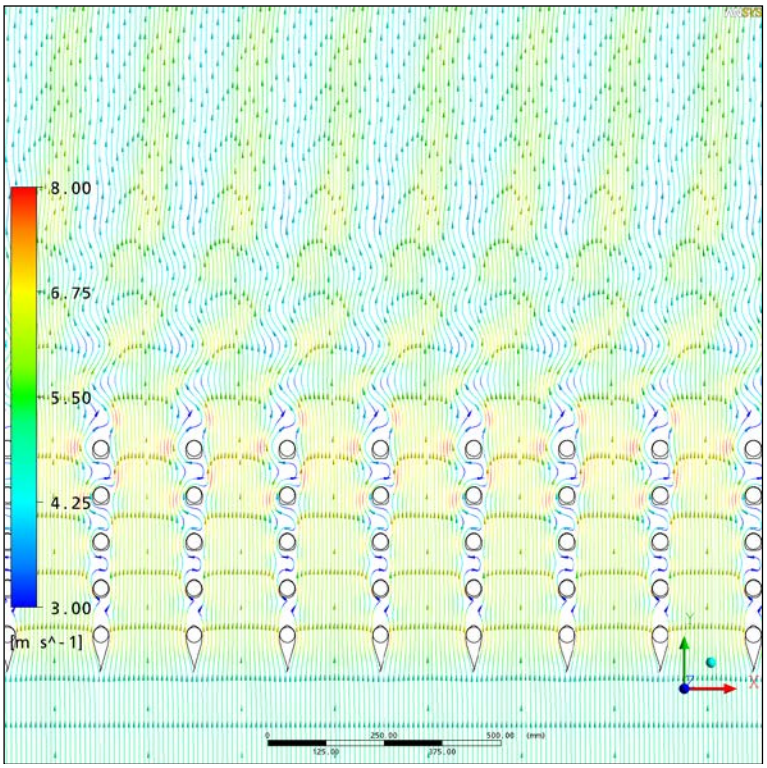

Fig. 5.5 Flow field for tubes with deposit

5.1.2 Deposit

The deposit formation is achieved by means of mesh motion capabilities in CFX. An incoming particle presents a certain mass and volume. From the combination of impaction region, number fraction, mass and statistical distribution the deposit growth can be calculated.

5.1.2.1 Tube 1

The main deposit formation mechanisms differ for the first, second and rest of tubes.
At the first tube the main effect is the impaction of coarse particles to the windward side.
Interesting is the formation at the lee side.

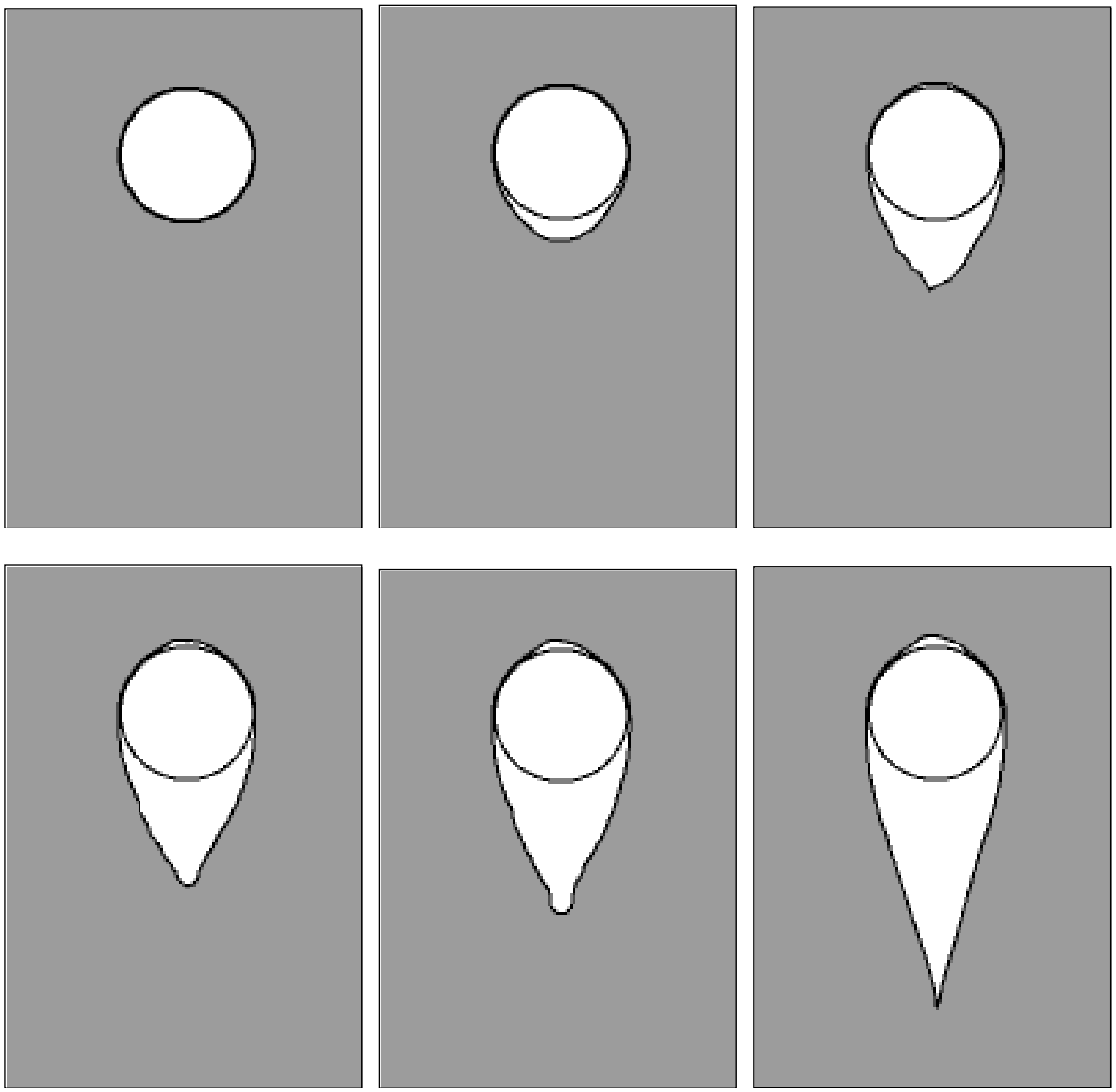

Fig. 5.6 Deposit growth for the 1st tube

With another illustration it is possible to detect the influence of different particle classes. Exemplary 6 of the 19 particle size classes are shown. The negative values represent the character of a sink to the flow field.

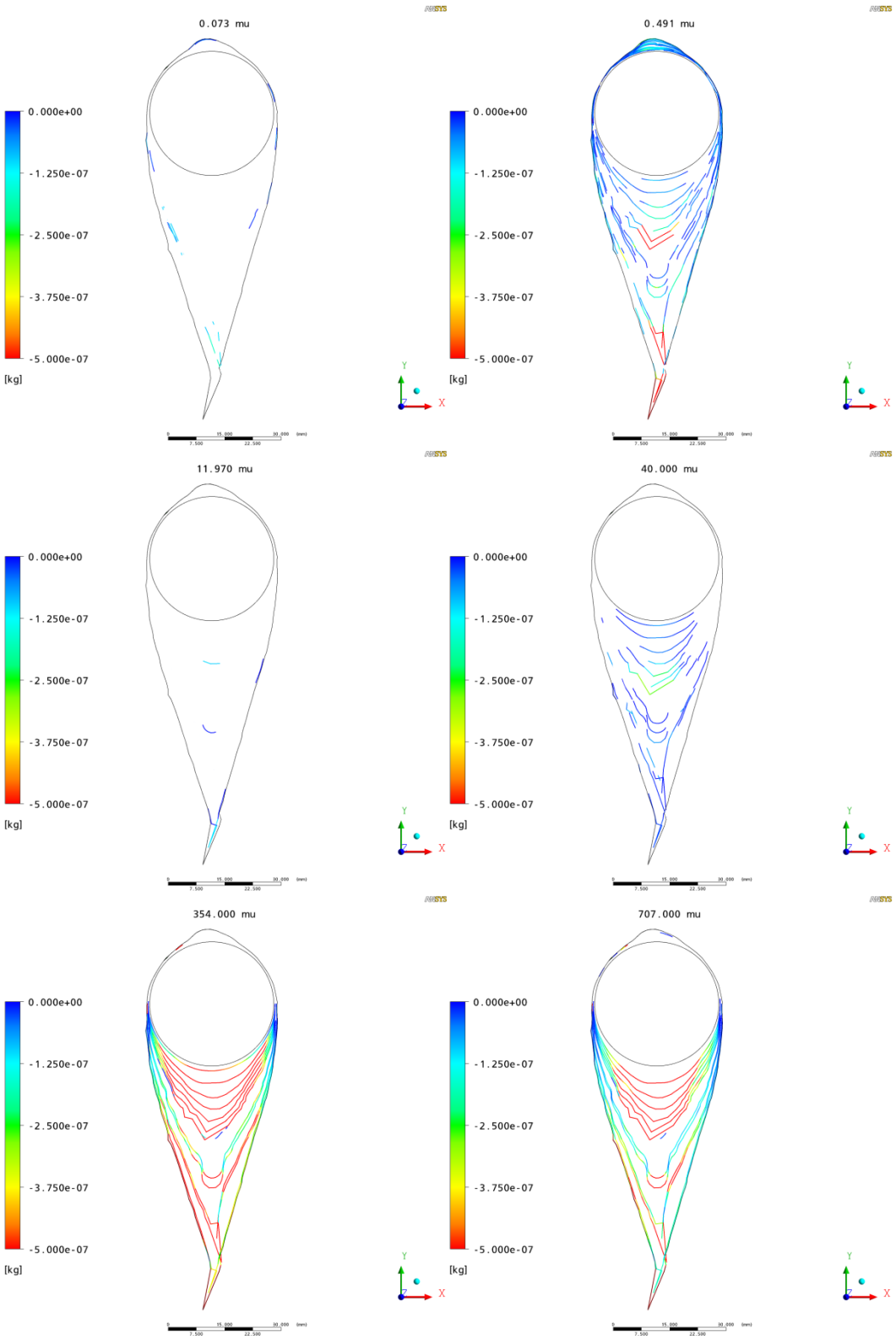

Fig. 5.7 Particle masses for several particle classes

The most important particles classed for the 1st row of tubes are the coarse particle above 500 µm. A significant part is also formed by particles of 0.491 µm, as this is the 1st peak in the bimodal particle distribution of the particles in flight.
In illustration 2 it is shown, that the deposit at the lee-side is exclusively formed by particles of 0.491 µm. On looking to the transient behaviour, which cannot be shown in this static report, it can be seen, that this particle are transported to the region between tube 1 and 2 and will then settle by gravitation.

5.1.2.2 Tube 2

As mentioned above tube 2 has an exceptional position, as the Karman-vortices have not build up and the tube is in the lee of tube 1.

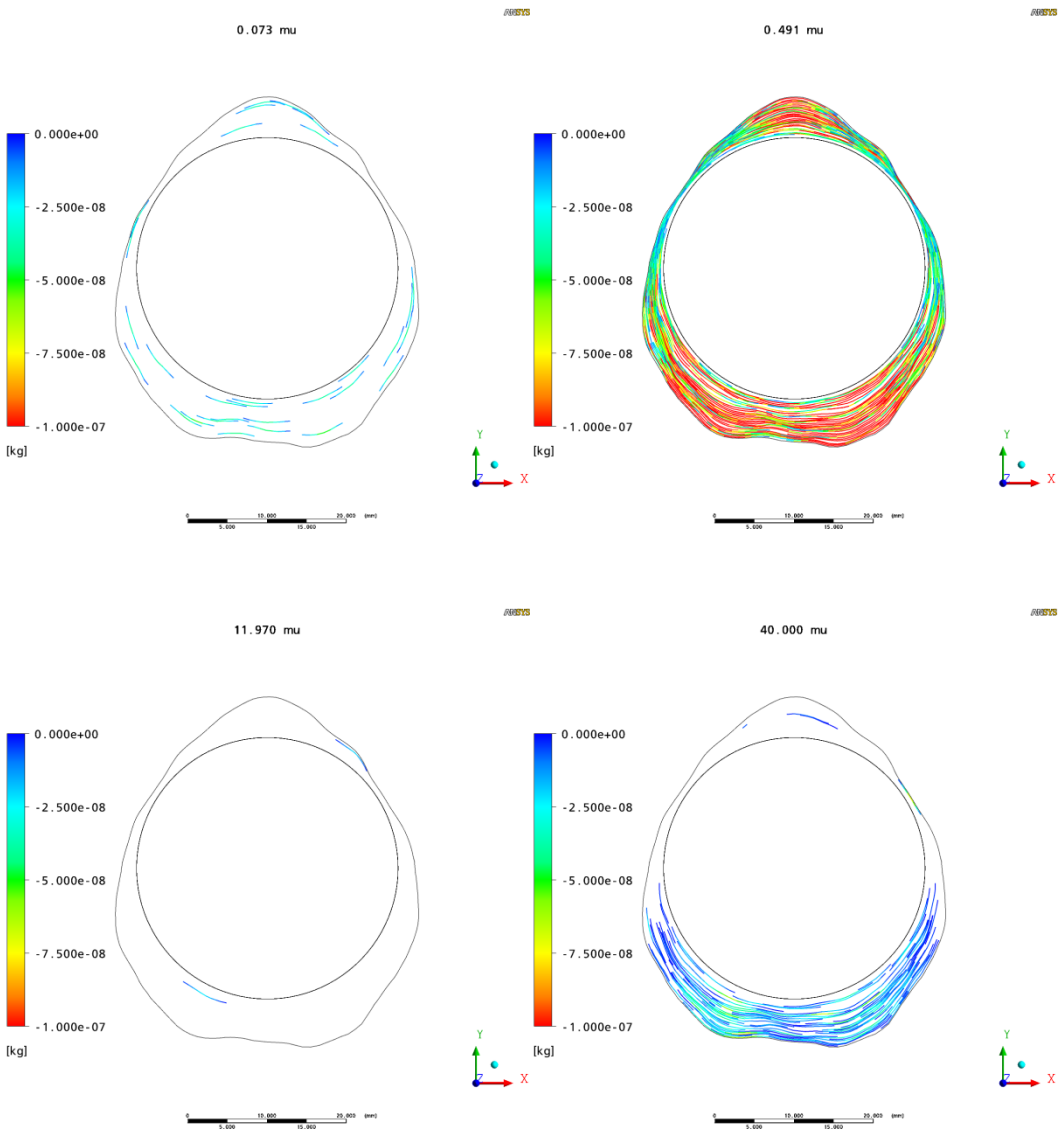

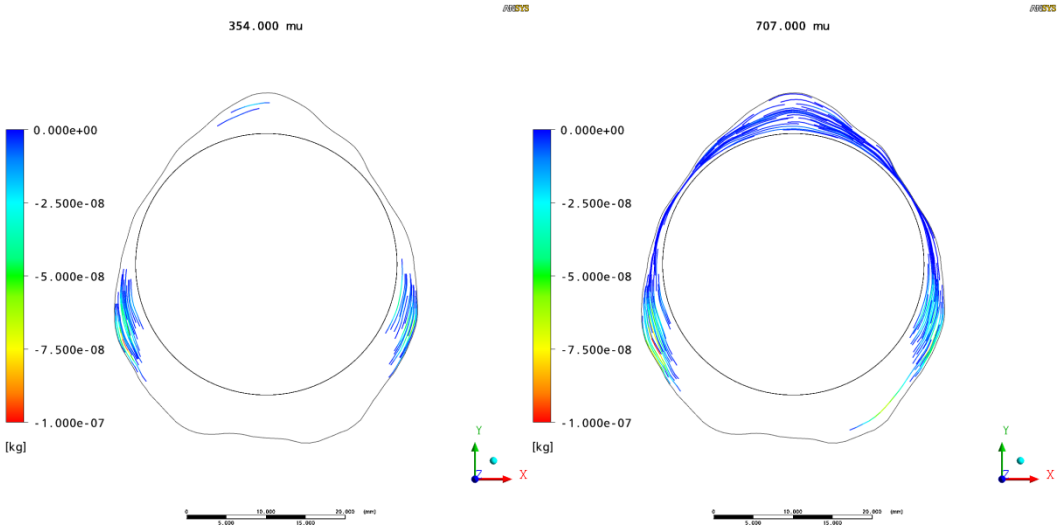

Fig. 5.8 Particle masses for several particle classes

The significant particle class is 0.491 µm. The driving effects will be turbulent fluctuations and thermophoresis. Interesting is the separation of particles at 707 µm to coarser ones. The 707 µm particles are deposit at the windward side whereas the greater ones are found at the rest of the tube.

5.1.2.3 Backmost tubes

The windward side of the deposit represents the bimodal character of the original dust. The lee side is formed almost only by the 0.491 µm particles.

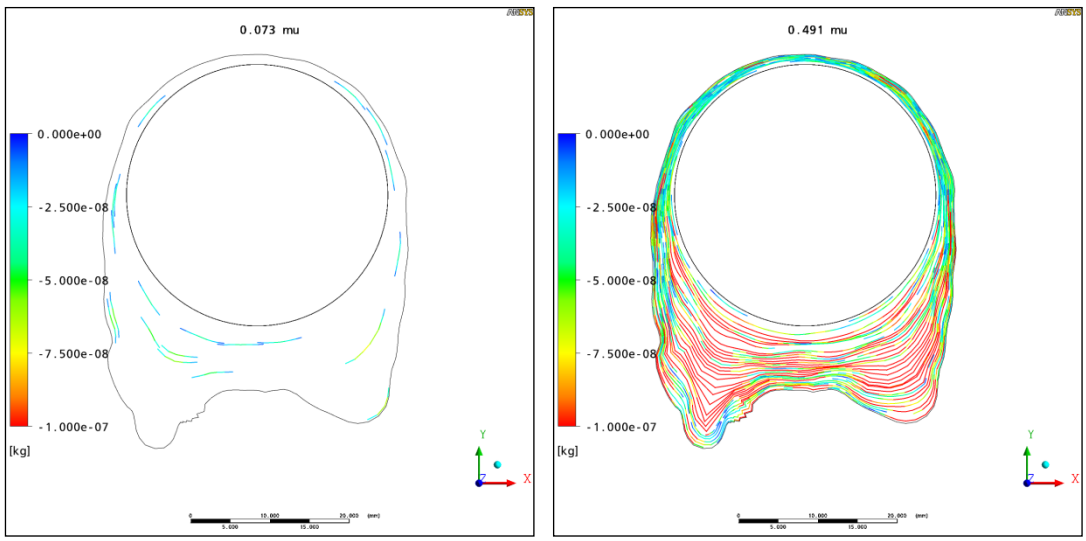

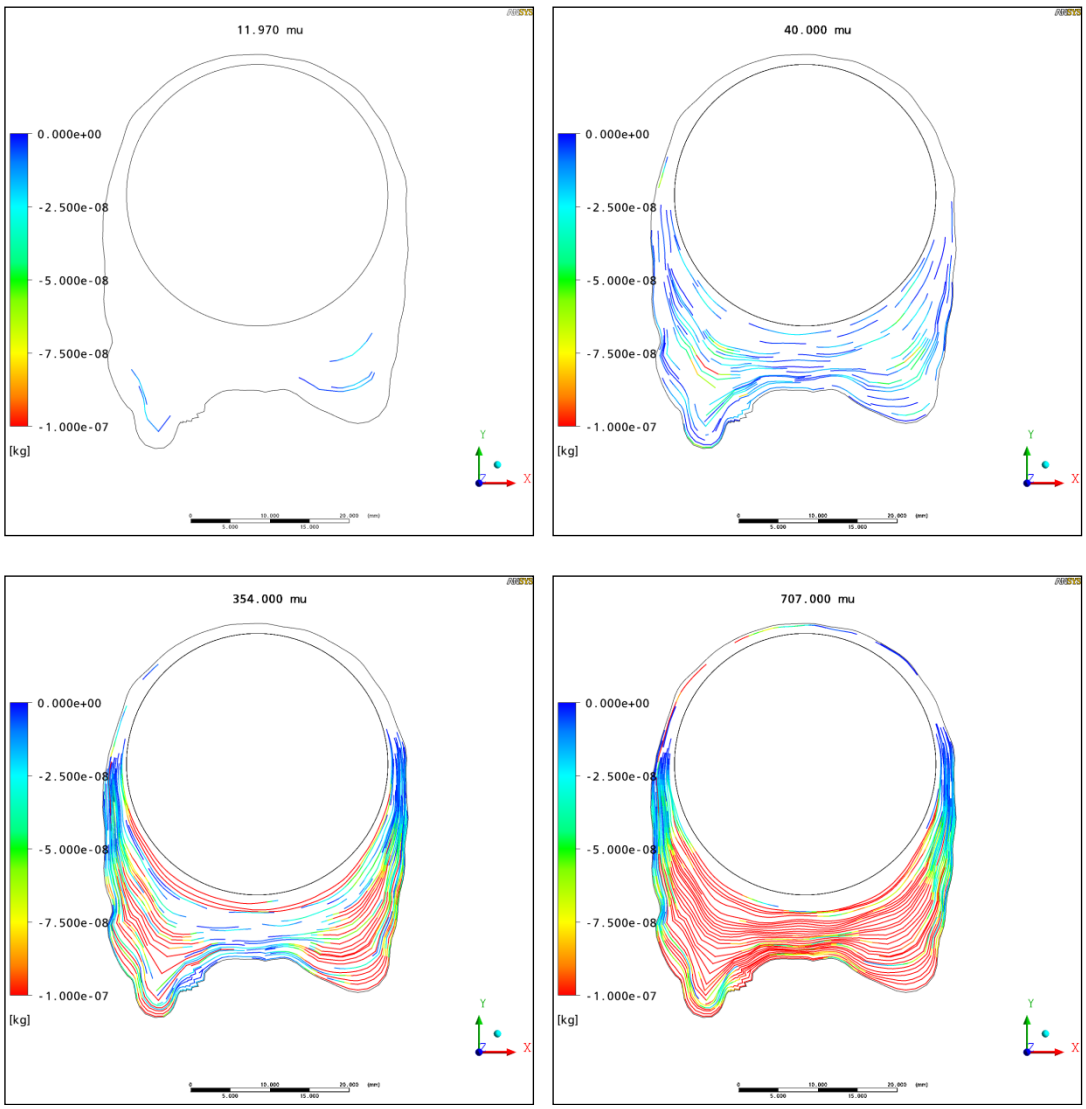

Fig. 5.9 Particle masses for several particle classes

5.1.2.4 General

The simulation shows, that the original bimodal distribution is not found in general for the deposit (Fig. 5.10), although a less significant bimodal distribution could be seen. Compared to the mass of deposits observed in the real plant at the superheaters 5 and 6 we found, that the real plant has a decreased amount of deposits. The decrease from calculated to real masses is about 63 %. This can be caused on the one hand by a lower sticking factor than assumed and on the other hand by the effect of the soot blowers.
All these results will give new insight to the corrosion processes.

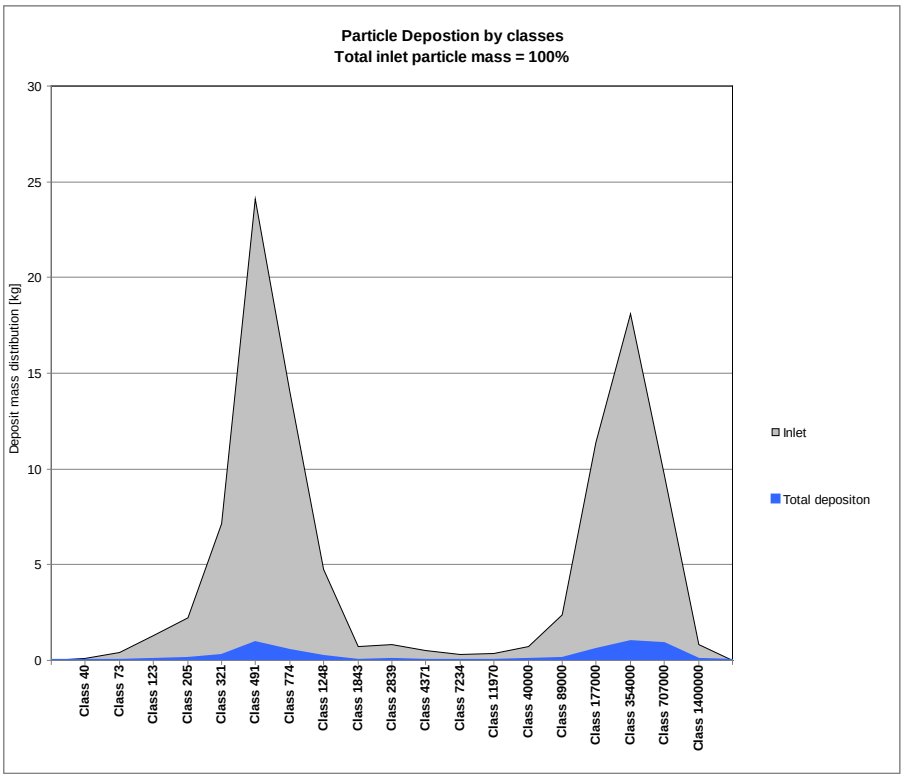

Fig. 5.10 Particle masses at inlet and deposit by classes

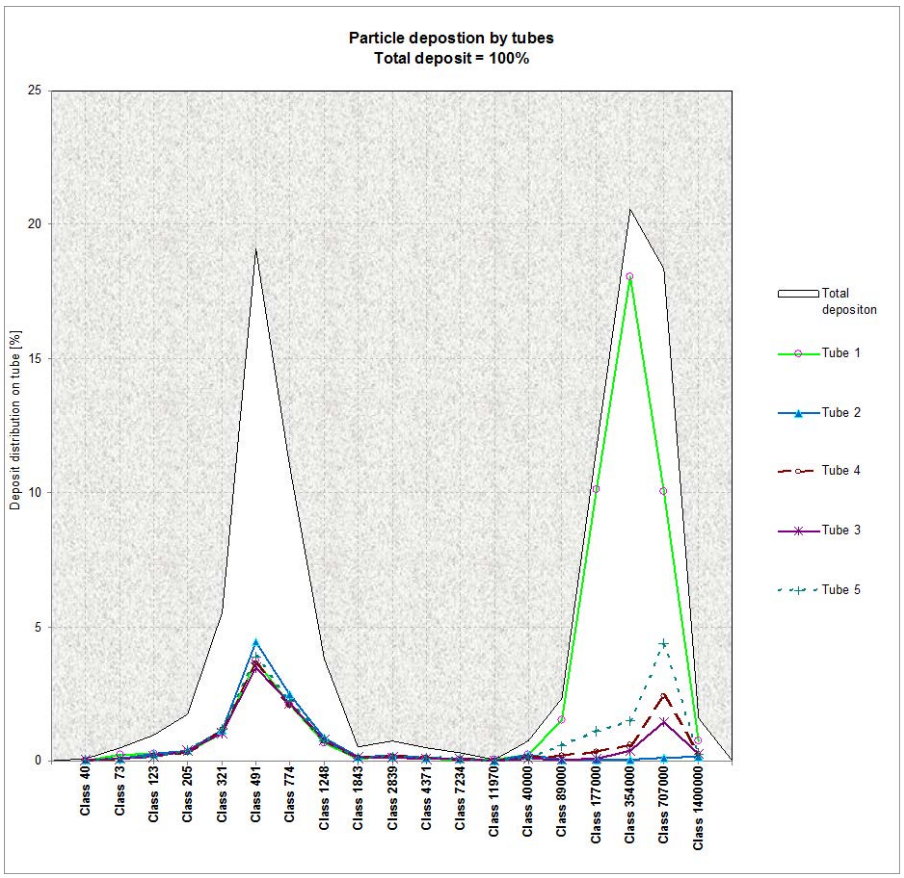

Fig. 5.11 Particle masses and deposit on individual tubes

5.1.2.5 Transient effect

As mentioned above the deposit formation is fully coupled to the flow field. This has 2 fundamental effects, the geometry will change and due to the thermal conductivity in the growing deposit the temperatures will change. The diagrams Fig. 5.12 and Fig. 5.13 show the temporal fluctuations.

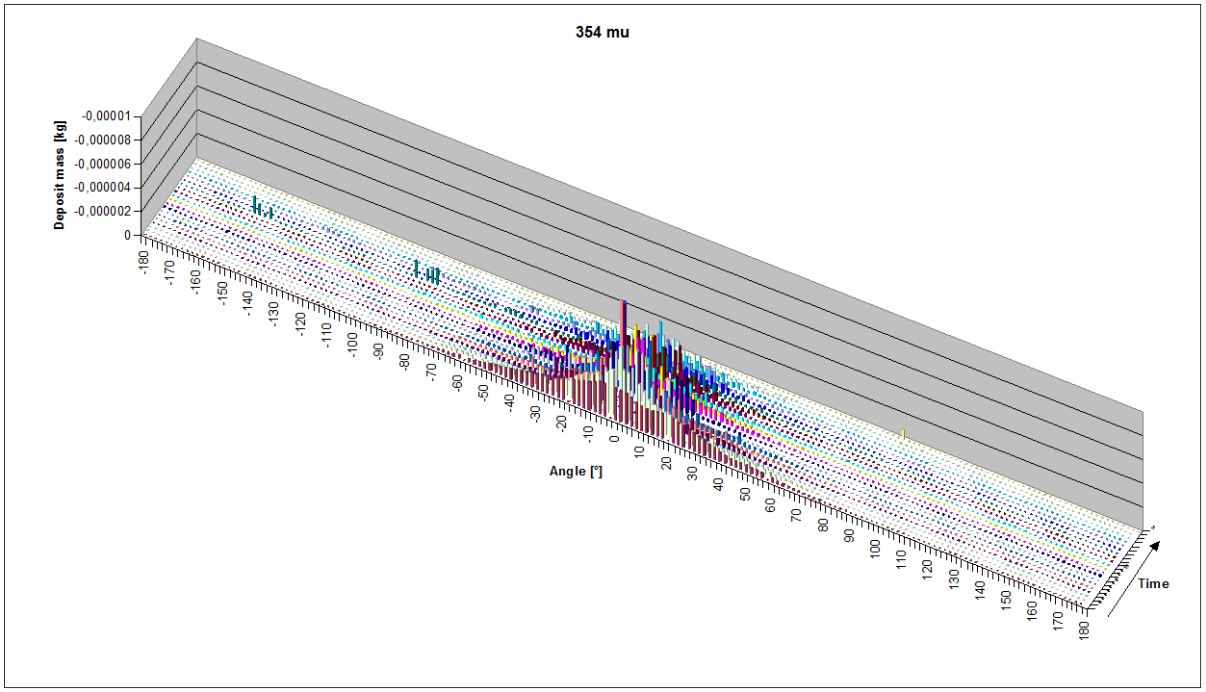

Fig. 5.12 Particle class 354 µm at the 1st tube

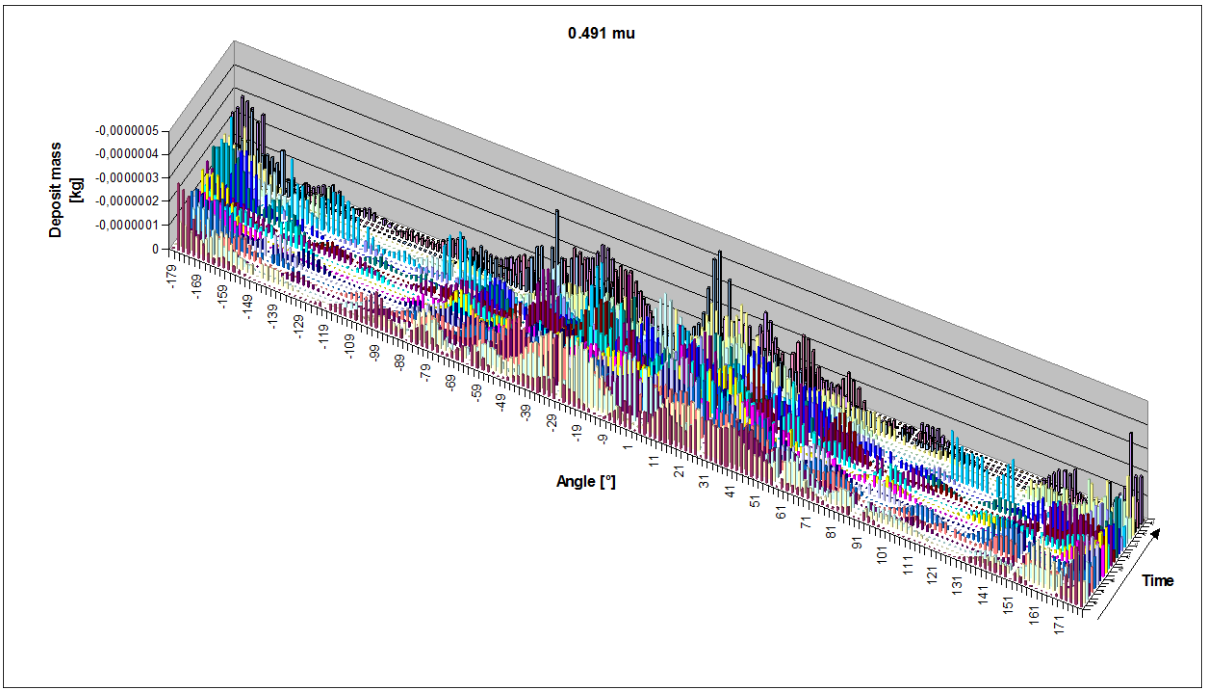

Fig. 5.13 Particle class 0,491 µm at the 2st tube

In Fig. 5.12 it can be seen, that the impact to the stagnation-point will decrease by time down to less than a half. Fig. 5.13 shows a more statistical deviation to average impact regions.

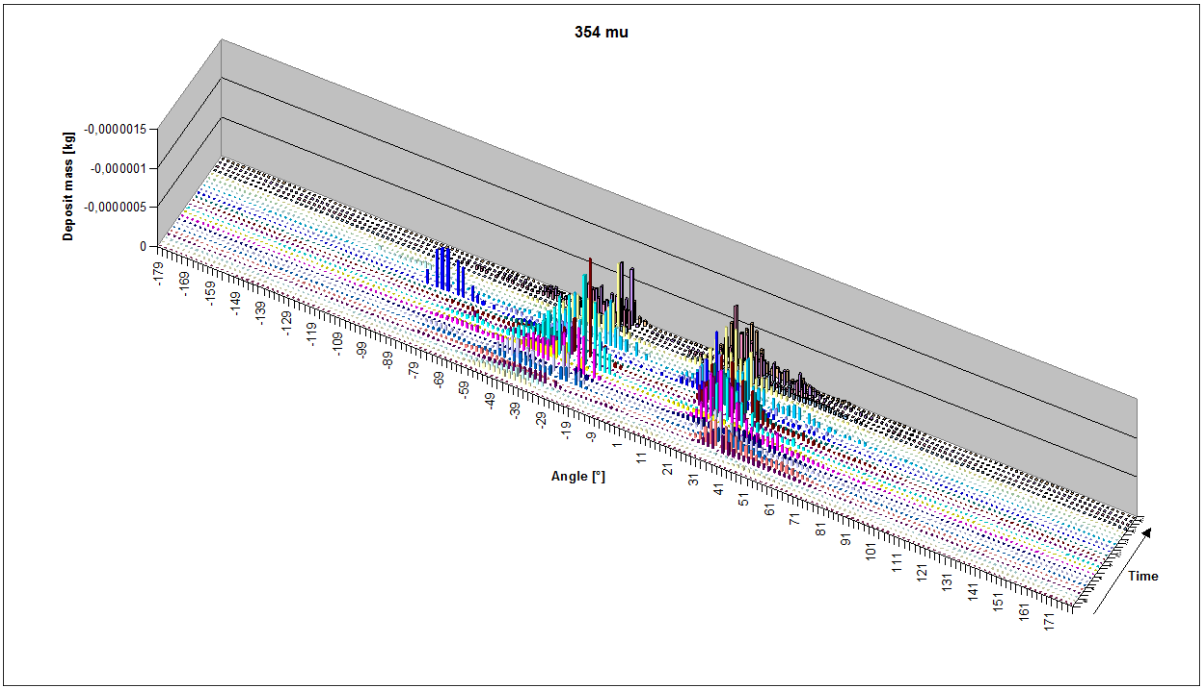

Fig. 5.14 Particle class 354 µm at the 5st tube

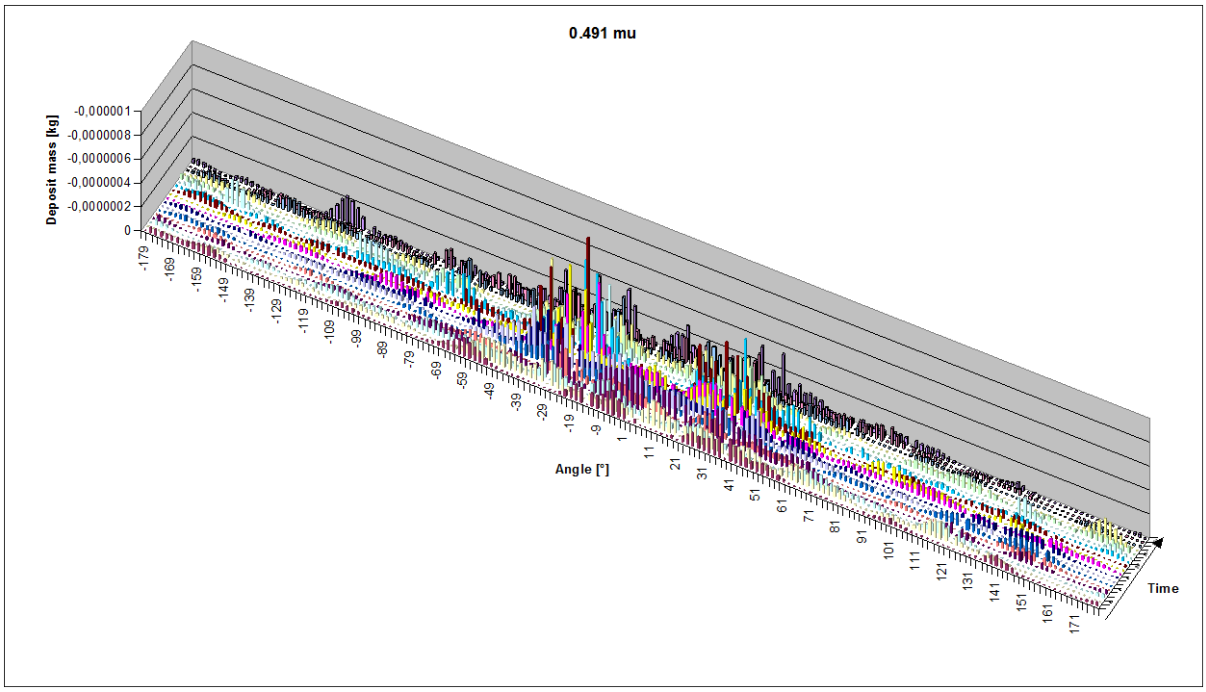

Fig. 5.15 Particle class 0.491 µm at the 5st tube

The intensive coupling between deposition, flow field and impact-probability is shown Fig. 5.14.

At the beginning there is no impact of 354 μm particle to that tube. But with the formation of the deposit the geometry becomes more and more appropriate to trapping rough particle. Whereas the fine particle deposition (Fig. 5.15) will smooth from a windward favoured absorption to an almost equal around the tube.

6 SUMMARY AND OUTLOOK

The presented works show the feasibility for calculation of formed detailed deposits. Although there is a limited knowledge to fundamental effects like e.g. sticking probability the results show excellent match to observed effects.

So the basis for further investigation of global and local corrosion is set. Open questions are still the initial formation of particles and the growth by condensation and agglomeration. The wide area around sticking, adhesion and interception has to be concerned.
Besides this “mechanical” prospect the chemical and diffusive kinetics will bring a new issue to the complex matter.

7 LITERATURE

[Deuerling, 2005] Deuerling, C., Maguhn, J., Nordsieck, H., Zimmermann, R., Warnecke, R.: Gas- und Aerosoldynamik in Leerzügen von MVA. VDI-Wissensforum (Hrsg.): Beläge und Korro-sion in Großfeuerungsanlagen beim Einsatz Heizwert- und Schadstoffreicher Fraktio-nen –Seminar am 14.-15. Juni 2005 in Hannover. VDI-Verlag, Düsseldorf, 2005

[Deuerling, 2009] Deuerling, Chr.: Untersuchungen zum Einfluss von Rauchgas-Aerosolen in Müll- und Biomasse-Verbrennungsanlagen auf die Hochtemperatur-Korrosion der Überhitzer, PhD Thesis, Rostock University (2009)

[Fuchs, 1964] Fuchs, N.A., The Mechanics of Aerosols, Pergamon Press (1964).

[Hinds, 1982] Hinds, W.C., Aerosol Technology, John Wiley (1982)

[Kaer, 2001] Kaer, S.K., Numerical Investigation of Deposit Formation in Straw-Fired Boilers, PhD Thesis, Aalborg University (2001)

[Koch, 1996] Koch, W., Über die Koagulation von Aerosolen und ihre Bedeutung für Umwelt und Verfahrenstechnik, Habilitationsschrift TU-Clausthal (1996)

[Löffler, 1988] Löffler, F., Staubabscheiden, Thieme (1988)

[Mikannen, 1999] Mikkanen, P.; Kauppinen, E. I.; Pyykönen, J.; Aurela, M; Vakkilainen, E. K.; Janka, K. (1999): Alkali Salt Ash Formation in Four Finnish Industrial Recovery Boilers. Energy & Fuels, 13: 778-795

[Obernberger, 2004] Obernberger, I.; Brunner, Th.: Deposition und Korrosion in Biomassefeuerungen. In: VDI-Wissensforum (Hrsg.): Beläge und Korrosion in Großfeuerungsanlagen – Seminar am 04.-05. Mai 2004 in Göttingen. Düsseldorf: VDI-Verlag, 2004

[Strand, 2004] Strand, M.; Bohgard, M.; Swietlicki, E.; Gharibi, A.; Sanati, M. (2004): Laboratory and field test of a sampling method for characterization of combustion aerosols at high tem-peratures. Aerosol Science & Technology 38 (8): 757-765

[Tran, 2002] Tran, K. Q.; Steenari, B. M.; Abul-Milh, M. (2002): Gas quenching probe and field meas-urements of gaseous cadmium in a 12-MWth circulating fluidised bed combustion boiler. Fuel 81 (13): 1647-1654

[Warnecke, 1999] Warnecke, R., Messungen an unterschiedlichen Messebenen in Feuerraum und 1. Zug der Linien 1 und 3 einer MVA. Würzburg: Noell - Interner Bericht (1999)

